



New insights into the early evolution of horizontal spiral trace fossils and the age of the Brioverian series (Ediacaran–Cambrian) in Brittany, NW France

Romain Gougeon, Didier Néraudeau, Alfredo Loi, Marc Poujol

► To cite this version:

Romain Gougeon, Didier Néraudeau, Alfredo Loi, Marc Poujol. New insights into the early evolution of horizontal spiral trace fossils and the age of the Brioverian series (Ediacaran–Cambrian) in Brittany, NW France. *Geological Magazine*, 2022, 159 (7), pp.1284-1294. <10.1017/S0016756820001430>. <insu-03124898>

HAL Id: insu-03124898

<https://insu.hal.science/insu-03124898v1>

Submitted on 31 Aug 2022

HAL is a multi-disciplinary open access archive for the deposit and dissemination of scientific research documents, whether they are published or not. The documents may come from teaching and research institutions in France or abroad, or from public or private research centers.

L'archive ouverte pluridisciplinaire **HAL**, est destinée au dépôt et à la diffusion de documents scientifiques de niveau recherche, publiés ou non, émanant des établissements d'enseignement et de recherche français ou étrangers, des laboratoires publics ou privés.



HAL Authorization

New insights on the early evolution of horizontal spiral trace fossils and the age of the Brioverian (Ediacaran-Cambrian) in Brittany, NW France

Journal:	<i>Geological Magazine</i>
Manuscript ID	GEO-20-2562.R3
Manuscript Type:	Original Article
Date Submitted by the Author:	n/a
Complete List of Authors:	Gougeon, Romain; University of Saskatchewan, Geological Sciences Neraudeau, Didier; Université de Rennes 1, Institut de Géologie Loi, Alfredo; Università di Cagliari, Dipartimento di Scienze Chimiche e Geologiche Poujol, Marc; Université de Rennes 1, Géosciences Rennes
Keywords:	U-Pb dating, Ichnology, Planispiral, Ediacaran-Fortunian, <i>Spirodesmos</i>
Abstract:	<p>In northwestern France, the Brioverian is a thick siliciclastic succession deposited during the Cadomian cycle (c. 750–540 Ma). In the uppermost Brioverian beds, previous studies unraveled an assemblage dominated by simple horizontal trace fossils associated with microbially-stabilized surfaces. Here, we report <i>Spirodesmos</i> trace fossils—one-way, irregular and regular horizontal spirals—from Crozon (Finistère, Brittany), Montfort-sur-Meu and St-Gonlay (Ille-et-Vilaine, Brittany). After reviewing the literature on horizontal spiral trace fossils from the Ediacaran to the Recent, an Ediacaran-Fortunian <i>Spirodesmos</i> pool is identified from marginal-marine to shelf settings, while an Ordovician-Recent trend formed in the deep-marine realm. These results suggest that an onshore-offshore migration in <i>Spirodesmos</i> took place from the Ediacaran-Fortunian to the Ordovician, similarly to what happened in graphoglyptids. In addition, the age of the uppermost Brioverian beds (Ediacaran or early Cambrian) is still a pending question. Here, we report two new U-Pb detrital zircon dating from sandstone samples in St-Gonlay, giving maximum deposition ages of 551 ± 7 Ma and 540 ± 5 Ma. Although these results do not discard an Ediacaran age for the uppermost Brioverian beds, a Fortunian age is envisioned because the new dating corroborate previous dating from Brittany, Mayenne and Normandy. However, the intervals of error of the radiometric dating, and the dominance of non-penetrative trace fossils associated with matgrounds (an ecology more typical of the Ediacaran), do not allow definitive conclusions on the age of the uppermost Brioverian beds.</p>

SCHOLARONE™
Manuscripts

1
2
3
4
5
6
7
8
9
10
11
12
13
14
15
16
17
18
19
20
21
22
23
24
25
26
27
28
29
30
31
32
33
34
35
36
37
38
39
40
41
42
43
44
45
46
47
48
49
50
51
52
53
54
55
56
57
58
59
60

Title: New insights on the early evolution of horizontal spiral trace fossils and the age of the
Brioverian (Ediacaran-Cambrian) in Brittany, NW France

Category of submission: Original Article (Special Issue on the Ediacaran-Cambrian
transition)

Authors: Romain Gougeon^{1,2}, Didier Néraudeau², Alfredo Loi³ and Marc Poujol²

Affiliations:

¹Department of Geological Sciences, University of Saskatchewan, Saskatoon, SK, S7N 5E2,
Canada

²Univ Rennes, CNRS, Géosciences Rennes - UMR 6118, F-35000 Rennes, France

³Dipartimento di Scienze Chimiche e Geologiche, Università di Cagliari, Cittadella
Universitaria, 09042 Monserrato, Italy

Short title: Early evolution of horizontal spiral trace fossils

Corresponding author: gougeon.romain@gmail.com

Abstract: In northwestern France, the Brioverian is a thick siliciclastic succession deposited during the Cadomian cycle (*c.* 750–540 Ma). In the uppermost Brioverian beds, previous studies unraveled an assemblage dominated by simple horizontal trace fossils associated with microbially-stabilized surfaces. Here, we report *Spirodesmos* trace fossils—one-way, irregular and regular horizontal spirals—from Crozon (Finistère, Brittany), Montfort-sur-Meu and St-Gonlay (Ille-et-Vilaine, Brittany). After reviewing the literature on horizontal spiral trace fossils from the Ediacaran to the Recent, an Ediacaran-Fortunian *Spirodesmos* pool is identified from marginal-marine to shelf settings, while an Ordovician-Recent trend formed in the deep-marine realm. These results suggest that an onshore-offshore migration in *Spirodesmos* took place from the Ediacaran-Fortunian to the Ordovician, similarly to what happened in graphoglyptids. In addition, the age of the uppermost Brioverian beds (Ediacaran or early Cambrian) is still a pending question. Here, we report two new U-Pb detrital zircon dating from sandstone samples in St-Gonlay, giving maximum deposition ages of 551 ± 7 Ma and 540 ± 5 Ma. Although these results do not discard an Ediacaran age for the uppermost Brioverian beds, a **Fortunian age** is envisioned because the new dating corroborate previous dating from Brittany, Mayenne and Normandy. However, **the** intervals of error of **the** radiometric dating, and the dominance of non-penetrative trace fossils associated with matgrounds (an ecology more typical of the Ediacaran), do not allow definitive conclusions on the age of the uppermost Brioverian beds.

Keywords: Ediacaran-Fortunian, ichnology, planispiral, *Spirodesmos*, U-Pb dating

1
2
3
4
5
6
7
8
9
10
11
12
13
14
15
16
17
18
19
20
21
22
23
24
25
26
27
28
29
30
31
32
33
34
35
36
37
38
39
40
41
42
43
44
45
46
47
48
49
50
51
52
53
54
55
56
57
58
59
60

1. Introduction

The potential of ichnology to decipher macro-evolutionary trends in animal behavior has a long history. Compilation of ichnological data was a major part of the work of A. Seilacher and P. Crimes. Seilacher (1974, 1977, 1986) focussed on the variety of graphoglyptid trace fossils from the deep-sea (i.e. patterned trace fossils forming nets, regular meanders and spirals), aiming to understand their environmental adaptation through time (e.g. size changes, functional optimization). Seilacher (1956) was the first to recognize the potential of trace fossils to delineate the Precambrian-Cambrian boundary; Crimes (1987, 1992*a*, 1994) extended this idea by reviewing worldwide literature, and developed an ichnostratigraphic scheme that helped defining the Cambrian GSSP (Narbonne *et al.* 1987; Brasier *et al.* 1994). In Crimes' comprehensive work, horizontal spiral trace fossils (as defined in this contribution) were consistently absent from the Ediacaran and the Cambrian (Crimes, 1987, 1992*a*, 1992*b*, 1994), only appearing by the Ordovician in the deep-marine realm (Crimes *et al.* 1974, 1992). Crimes suspected that most deep-marine graphoglyptids originated in shallow-marine environments during the Cambrian (Crimes, 1987; Crimes & Anderson, 1985; Crimes & Fedonkin, 1994), but the absence of regular planispiral trace fossils in the Cambrian was then problematic (Crimes *et al.* 1992).

The Ediacaran-Cambrian transition (c. 539 Ma) was a time of striking changes in Earth ecosystems. Ediacaran seafloors were dominated by microbially-stabilized surfaces on which epifaunal and very shallow infaunal grazers thrived (Seilacher & Pflüger, 1994; Gehling, 1999). Macroscopic animals of the earliest Cambrian started to disrupt the sediment at depth, affecting the substrate ventilation (e.g. Mángano & Buatois, 2014; Gougeon *et al.* 2018*a*), trophic webs (e.g. Bottjer *et al.* 2000; Meysman *et al.* 2006), and geochemical cycles (e.g. Logan *et al.* 1995; Canfield & Farquhar, 2009; Boyle *et al.* 2018). In northwestern France, the Brioverian of central Brittany is a thick siliciclastic succession that was deposited

1
2
3 61 during the Cadomian cycle (*c.* 750–540 Ma). Despite the report of fossils since the 19th
4
5 62 century, the age of its uppermost beds (Ediacaran or early Cambrian) is a long-standing
6
7 63 conundrum. Recently, new investigations unraveled a unique assemblage of trace and body
8
9 64 fossils in the vicinity of Rennes (Néraudeau *et al.* 2016, 2019; Gougeon *et al.* 2018b, 2019).
10
11
12 65 Trace fossils are dominantly simple, horizontal, and associated with microbially-stabilized
13
14 66 surfaces; of these, planispirals stand as a surprising discovery.
15
16

17
18 67 The aim of this study is threefold: (1) to describe a new assemblage of planispiral trace
19
20 68 fossils from the Brioverian of northwestern France; (2) to place this assemblage within a
21
22 69 macro-evolutionary framework, and to interpret its significance; and (3) to provide new
23
24 70 radiometric dating, in order to discuss the age of the uppermost Brioverian deposits.
25
26

27 71 **2. General background**

28 72 **2.a. Geological setting and previous work**

29
30
31
32
33 73 The Brioverian (*c.* 660–540 Ma; Le Corre *et al.* 1991; Guerrot *et al.* 1989, 1992) is an
34
35 74 informal name given to a thick sedimentary succession deposited during the Cadomian cycle
36
37 75 (*c.* 750–540 Ma) in northwestern France (Fig. 1a, b; Chantraine *et al.* 2001; Ballèvre *et al.*
38
39 76 2013). In the Rennes area (Fig. 1b), only the uppermost Brioverian beds are exposed, with a
40
41 77 thickness evaluated at *c.* 1300 m (Trautmann *et al.* 1999). The Brioverian of Brittany lies
42
43 78 unconformably on an Icartian basement (*c.* 2200–1800 Ma) and is unconformably overlain
44
45 79 either by the Ordovician Red Bed Series (‘Séries Rouges Initiales’) or by the Ordovician
46
47 80 Armorican Sandstone (‘Grès Armoricaïn’; Cogné, 1959; D’Lemos *et al.* 1990; Le Corre *et al.*
48
49 81 1991). The terrigenous siliciclastic sediments of the Brioverian resulted from the erosion of
50
51 82 the Cadomian belt in northern Brittany and accumulated in a marginal, intra-plate basin in
52
53 83 central Brittany (Denis, 1988; Dissler *et al.* 1988; Rabu *et al.* 1990; Dabard *et al.* 1996).
54
55 84 Locally, carbonaceous cherts (‘phtanites’), limestones, and igneous intrusions have also been
56
57
58
59
60

reported (Denis & Dabard, 1988; Dabard, 1990, 2000; Chantaine *et al.* 2001). On a regional scale, the correlation of the Brioverian sedimentary deposits is hindered by the discontinuous outcropping, facies changes, the absence of biostratigraphic markers, and the metamorphic overprint from the Devonian-Carboniferous Variscan orogeny (Denis & Dabard, 1988; D'Lemos *et al.* 1990; Le Corre *et al.* 1991; Ballèvre *et al.* 2013). While traditionally interpreted as deeper-marine turbiditic deposits (Dangeard *et al.* 1961; Denis, 1988; Trautmann *et al.* 1999), the Brioverian sedimentary beds also show evidence of shallow-marine storm-influenced (Dabard & Loi, 1998; Dabard & Simon, 2011) and marginal-marine tidally-influenced conditions (Graindor, 1957; Dabard, 1990, 2000; Néraudeau *et al.* 2019).

[insert Figure 1]

Fossils recovered from the Brioverian are algal or bacterial organic-walled microfossils in cherts and limestones (Cayeux, 1894; Deflandre, 1955; Chauvel & Schopf, 1978; Chauvel & Mansuy, 1981; Mansuy & Vidal, 1983), macroscopic body fossils of unknown origin (Néraudeau *et al.* 2019), and trace fossils. Ichnofossils were first discovered in the late 19th century (Lebesconte, 1886), but did not draw the attention of the scientific community for a long time. Recently, new investigations in the vicinity of Rennes (Fig. 1b) have unraveled an assemblage dominated by simple horizontal grazing trails (*Circulichnis*, *Gordia*, *Helminthoidichnites*, *Helminthopsis*), passively-filled horizontal burrows (*Palaeophycus*), and horizontal spiral trace fossils (*Spirodesmos*; Néraudeau *et al.* 2016; Gougeon *et al.* 2018b, 2019). In addition, microbially-textured surfaces (MISS of Noffke *et al.* 2001) are common both in fossiliferous and azoic intervals (Lebesconte, 1886; Gougeon *et al.* 2018b).

The age of the uppermost Brioverian sedimentary beds in Brittany, Normandy, and Mayenne, has been highly debated (Fig. 1b). In Brittany, the overlying Red Bed Series gave an age of 472 ± 5 Ma (Rb-Sr dating from volcanic rocks; Auvray *et al.* 1980), 465 ± 1 Ma (U-

Pb dating from volcanic rocks; Bonjour *et al.* 1988; Bonjour & Odin, 1989), and 486 ± 28 Ma (Pb-Pb dating from volcanic rocks; Guerrot *et al.* 1992), placing these beds within the Ordovician period (*contra* McMahon *et al.* 2017; Went, 2017). In the westernmost part of Brittany (Crozon area; Fig. 1b), Guerrot *et al.* (1992) obtained an age of 543 ± 18 Ma (Pb-Pb dating) for a tuff intercalated within Brioverian beds, whereas a maximum deposition age of 546 ± 2 Ma (U-Pb dating) has been obtained by Ballouard *et al.* (2018) from detrital zircon grains extracted from a sandstone (see also Dabard *et al.* 2021). In the vicinity of Rennes (Fig. 1b), detrital zircon grains gave a maximum deposition age of *c.* 550 Ma (U-Pb dating from sandstone and siltstone; Gougeon *et al.* 2018b); however, five zircon grains, dated at 532.1 ± 3.9 Ma, were problematic to interpret (Gougeon *et al.* 2018b). In Normandy, Brioverian sediments were deposited in a different palaeogeographic domain than in central Brittany, as they are separated by the North-Armorican Shear Zone (Fig. 1b; Chantaine *et al.* 1982; Guerrot *et al.* 1992). In this domain, granitoid intrusions within Brioverian sediments have been dated at 540 ± 10 Ma (U-Pb dating on monazite; Pasteels & Doré, 1982). In Mayenne, where the Brioverian is in continuity with its equivalent of central Brittany (Fig. 1b), radiometric dating on zircon grains yielded an age of 540 ± 17 Ma (tuff and detrital horizons; Guerrot *et al.* 1992).

2.b. Outcrops under study and depositional environments

The outcrop at 'La Lammerrais' village nearby St-Gonlay (Fig. 1b) yields slates with trace fossils, stacked in a pile about two metres high and fifty metres long (outcrops for this contribution are located on private properties, which do not allow details on their exact locations). These slates were extracted from a pit that was exploited by locals to build houses and pathways decades ago; unfortunately, the pit is now covered with vegetation and therefore impossible to sample *in situ*. Slates are made of siltstone and rare very fine- to fine-grained sandstone. One loose sandstone sample was collected for U-Pb dating, coming from a

135 nearby agricultural field. At ‘La Lammerais’ outcrop, sedimentary structures are parallel-
136 lamination organised in siltstone-sandstone bundles (i.e. rhythmite-like; Néraudeau *et al.*
137 2019, fig. 3), current-ripples (Néraudeau *et al.* 2019, fig. 2), tool-marks/spindle-shaped flute-
138 marks, possible load-casts, and pustular and wrinkled microbially-textured surfaces (Gougeon
139 *et al.* 2018b, figs 4, 7).

140 Nearby St-Gonlay, another outcrop has been investigated at ‘Le Lorinou’ village,
141 located 1.4 kilometres to the east of ‘La Lammerais’. This outcrop is very poor in trace fossils
142 (no spiral trace fossils were found there), but beds are preserved *in situ* and a sandstone
143 sample was collected for U-Pb zircon dating.

144 The outcrop of ‘Le Bois-du-Buisson’ is located at the entrance of a small forest in
145 Montfort-sur-Meu (Fig. 1b). It consists of a small quarry of about three metres high and ten
146 metres long, with vegetation extensively covering the sedimentary beds. However, a few
147 siltstone beds are accessible and reveal fresh surfaces with trace fossils. Sedimentary
148 structures are parallel-lamination organised in siltstone-sandstone bundles (i.e. rhythmite-like,
149 similarly to what is found at ‘La Lammerais’), and pustular and wrinkled microbially-
150 stabilized surfaces.

151 In addition, Montfort-sur-Meu is the host of ‘Les Grippeaux’ quarry, where P.
152 Lebesconte recovered fossils for the first time in the late 19th century (Lebesconte, 1886;
153 Gougeon *et al.* 2018b). Nowadays, the quarry is secured by a fence preventing any access.
154 Many samples were collected in the late 19th and early 20th century by P. Lebesconte, F.
155 Kerforne, and other geologists; they are housed at the Geological Institute of the University of
156 Rennes 1 and at the Museum of Natural History of Nantes, and are available for study.
157 Sedimentary structures are pustular microbially-stabilized surfaces.

The outcrop in Crozon (Fig. 1b) is located on the coastal cliff at ‘La Plage-du-Goulien’. This outcrop has not been visited by the authors, and the only trace fossil discovered was reported by E. Hanson in 2014 (pers. comm.). The sedimentology of the Brioverian from the Bay of Douarnenez and the Cove of Dinan (both in the vicinity of Crozon) has been studied in two doctoral theses (Darboux, unpubl. Ph.D. thesis, University of Brest, 1973; Denis, 1988). The succession displays parallel-laminated/bedded sandstone and siltstone with flute-casts, load-casts, tool-marks, rip-up clasts, carbonate concretions, normal and reverse grading, convolute bedding, flame structures, and current, wave, and climbing ripples. Both authors interpreted the succession as deposited by turbidites, located either below the limit of the storm wave-base action, or deeper in an abyssal plain. However, Denis (1988) noted the presence of oscillatory flow structures, lenticular bedding (Facies 3 of Denis, 1988) and mud-drapes, which are more typical of shallower environments.

In Montfort-sur-Meu and St-Gonlay, the dominance of siltstone intercalated with laminated very fine-grained sandstone, and the record of rhythmite-like bundles and current ripples, suggest a marginal-marine, tidally-influenced depositional environment (cf. Nio & Yang, 1991; Tessier *et al.* 1995; Dalrymple, 2010). This conclusion is strengthened by observations in Chanteloup and Nouvoitou (both in the vicinity of Rennes), where a sandstone facies displays mudstone drapes within fine-grained sandstone samples (i.e. flaser lamination; Supplementary Figure 1); these areas could represent the seaward, sandier part of the intertidal system. Sedimentary structures made by oscillatory flows (e.g. wave ripples, hummocky cross-stratification) have not been observed in the area so far. These conclusions are preliminary and await further support, notably from Brioverian outcrops revealing bedding architecture, and from more sampling of sedimentary structures.

3. Material and methods

3.a. Terminology of planispiral trace fossils

This contribution focusses only on spirals formed on a horizontal plane (i.e. planispirals). Three-dimensional, vertically (e.g. *Gyrolithes*, *Lapispira*) or horizontally (e.g. *Avetoichnus*, *Helicodromites*, *Helicolithus*) oriented spirals, are not comparable with the Brioverian material. In order to describe spiral morphologies, the following terms will be used: a *regular* spiral maintains a constant distance between whorls (Fig. 2b, c); an *irregular* spiral has a variable distance between whorls (Fig. 2a, d); a *one-way* spiral is a simple spiral with no central turnaround (Fig. 2a, b, d; Seilacher, 1977; Crimes & McCall, 1995); a *two-way* spiral is a double spiral with a central turnaround (Fig. 2c; Seilacher, 1977; Crimes & McCall, 1995); and a *bounded* spiral is an irregular, one-way spiral that decreases the distance between whorls outward (Fig. 2d).

[insert Figure 2]

3.b. U-Pb dating method

A classic mineral separation procedure has been applied to concentrate zircon grains for U-Pb dating. Rocks were crushed and only the powder fraction with a diameter < 250 µm was kept. Heavy minerals were successively concentrated by Wilfley table, heavy liquids, and with an isodynamic Frantz separator. Zircon grains were then handpicked under a binocular microscope to produce the most representative sampling, with the aim to avoid any intentional bias (see Malusà *et al.* 2013 and references therein). Selected grains were then embedded in epoxy mounts, grounded and polished. Zircon grains were imaged by cathodoluminescence (CL) using a Reliotron CL system equipped with a digital color camera available at the GeOHeLiS analytical platform (University of Rennes 1).

U-Pb geochronology was conducted by *in situ* laser ablation inductively coupled plasma mass spectrometry (LA-ICP-MS) at the GeOHeLiS analytical platform using an ESI NWR193UC Excimer laser coupled to a quadripole Agilent 7700x ICP-MS. Instrumental

conditions are reported in Supplementary Table S1, while the analytical protocol can be found in Manzotti *et al.* (2015). Kernel density diagrams for analyses that are $100 \pm 10\%$ concordant were generated using IsoplotR (Vermeesch, 2018). When dealing with detrital zircon geochronology, a minimum of 3 different ages obtained on 3 different zircon grains overlapping in age at 2σ has been demonstrated to produce a statistically robust maximum deposition age (Dickinson & Gehrels, 2009). The second important criteria in order to determine this maximum deposition age is the degree of concordance of the individual analysis used to calculate this age. Most authors consider all analyses that are 90% concordant or more, while others only analyses that are at least 95% concordant. In this study, because of the complexity of one of the data set ('La Lammerais'), only analyses that were at least 95% concordant were considered to calculate the maximum deposition age, in order to avoid using apparent ages that could be younger than the true age due to a non-negligible Pb loss.

3.c. Museum repository

From 'La Lammerais' and 'Le Bois-du-Buisson', samples were collected and repositied at the Geological Institute of the University of Rennes 1 (collections Gougeon and Néraudeau). Historical specimens from 'Les Grippeaux' are repositied at the Museum of Natural History of Nantes (collections Barrois and Lebesconte) and the Geological Institute of the University of Rennes 1 (collections Kerforne, Rolland and Rouault). The trace fossil from 'La Plage-du-Goulien' has not been collected and was only photographed in the field by E. Hanson.

4. Results

4. a. Planispiral trace fossils from the Brioverian

The Brioverian of central Brittany contains a rich assemblage of simple horizontal trace fossils, with *Helminthoidichnites* and *Helminthopsis* being the most common forms.

1
2
3
4
5
6
7
8
9
10
11
12
13
14
15
16
17
18
19
20
21
22
23
24
25
26
27
28
29
30
31
32
33
34
35
36
37
38
39
40
41
42
43
44
45
46
47
48
49
50
51
52
53
54
55
56
57
58
59
60

Originally, Lebesconte (1886, pl. 34, fig. 7) figured a planispiral trace fossil from Montfort-sur-Meu, without further discussion. Since then, spiral trace fossils have not been reported in the Brioverian. Here, we describe two types of planispiral trace fossils: (1) irregular, one-way spiral trace fossils; and (2) regular, one-way spiral trace fossils.

[insert Figure 3]

Four irregular, one-way spiral trace fossils were recovered from ‘La Lammerais’, ‘Le Bois-du-Buisson’, and ‘Les Grippeaux’ (Fig. 3a). Specimens are 0.3–1 mm wide, have 1¼–1¾ whorls, and are preserved in positive and negative reliefs (preservation as epirelief or hyporelief is unknown because slates with trace fossils are not preserved *in situ*). One specimen (Fig. 3a) has a different infill than the host rock and a lining; this is potentially a burrow. Rarely, they are associated with *Helminthoidichnites*, small-scale branching trace fossils (cf. *Pilichnus*), and pits of uncertain affinity. They are commonly found on pustular microbially-textured surfaces.

Two regular, one-way spiral trace fossils were recovered from ‘La Plage-du-Goulien’ and ‘Les Grippeaux’ (Fig. 3b, c). Specimens are 1–3 mm wide, have 2¼–2½ whorls, and are preserved in positive and negative reliefs. The distance between whorls remains constant until the last whorl, where the course detaches from the spiral system and progressively disappears. They are associated with *Helminthopsis* and pits of uncertain affinity. The surfaces they are found on are not textured.

Spirodesmos, *Spirophycus* and *Spirorhaphe* are the most common planispirals from the trace fossil record: however, their morphological boundaries are unclear. *Spirodesmos* is a regular to irregular, one-way spiral trace fossil (Geinitz, 1867; Andrée, 1920; Huckriede, 1952; Xia *et al.* 1987). For Seilacher (1977), *Spirodesmos* has a wide spacing between whorls; although this is clearly so in the type ichnospecies *S. interruptus* Andrée, 1920, *S.*

255 *archimedeus* Huckriede, 1952 has a narrower spacing between whorls. This issue becomes
 256 critical with *Spirodesmos kaihuaensis* Xia, He & Hu, 1987 and *S. spiralis* (Geinitz, 1867),
 257 both having irregular courses with variable distances between whorls. *Spirophycus* is a regular
 258 to irregular, one-way spiral trace fossil that commonly grades into meanders (Heer, 1876;
 259 Häntzschel, 1975). Seilacher (1977) argued that *Spirophycus* has wide strings with a
 260 tubercular surface and backfilled laminae (see also Książkiewicz, 1977; but see Uchman,
 261 1998). The spiral portion of *Spirophycus* (e.g. Heer, 1876, pl. 66, fig. b; Sacco, 1888, pl. 2,
 262 fig. 14), with regular whorls distinctly spaced from each other, can however be very similar to
 263 *Spirodesmos archimedeus*. *Spirorhaphe* is a regular to irregular spiral trace fossil with either a
 264 one-way (*S. azteca*, *S. graeca*) or two-way (*S. involuta*) course (Seilacher, 1977; Crimes &
 265 McCall, 1995). The inclusion of one-way spirals in *Spirorhaphe* is overlapping with
 266 *Spirodesmos* and *Spirophycus* morphologies, which is problematic.

267 Despite these taxonomical issues (see also Crimes & Crossley, 1991; Uchman, 1998;
 268 Minter & Braddy, 2009), planispirals from the Brioverian are comparable to *Spirodesmos*.
 269 Brioverian irregular, one-way spiral trace fossils are reminiscent of *Spirodesmos spiralis* (cf.
 270 Geinitz, 1867; Stepanek & Geyer, 1989). However, because of its irregular course and the
 271 poor extent of its whorls, *Spirodesmos spiralis* needs to be re-evaluated taxonomically; in this
 272 study, Brioverian forms are referred to *Spirodesmos* isp. Conversely, Brioverian regular, one-
 273 way spiral trace fossils belong to *Spirodesmos archimedeus* (cf. Huckriede, 1952; Zapletal &
 274 Pek, 1971; Horn, 1989). *Spirodesmos* ranges from the Ediacaran-Cambrian (this study) to the
 275 Holocene (e.g. Kitchell *et al.* 1978; Smith *et al.* 2005).

276 4.b. U-Pb dating

277 For the sandstone sample from 'La Lammerais', 118 zircon grains were analysed,
 278 among which 107 analyses have a concordance of $100 \pm 10\%$. Their U (49 to 1195 ppm) and
 279 Pb (6 to 493 ppm) contents, as well as their Th/U ratios (0.02 to 1), are highly variable

(Supplementary Table S2). A first group of 12 analyses yields apparent ages between 2.8 and 1.06 Ga. The remaining analyses form two major peaks at 600 Ma and 550 Ma, with minor peaks around 850 and 650 Ma (Fig. 1c). The 10 youngest analyses that are more than 95% concordant yield a weighted average $^{206}\text{Pb}/^{238}\text{U}$ date of 540 ± 5 Ma (MSWD = 1.2) that we consider as the maximum deposition age for this sandstone.

For the sandstone sample from ‘Le Lorinou’, 89 grains were analysed, out of which 68 are $100 \pm 10\%$ concordant (Supplementary Table S2). They are characterized by variable U and Pb contents (21 to 726 ppm and 2 to 242 ppm, respectively), with Th/U ratios between 0.05 and 1.4. A first group of 22 zircon grains yields Neoproterozoic (2.9 Ga) to Palaeoproterozoic ages (1.8 Ga), followed by a gap until the end of the Mesoproterozoic. The remaining grains present apparent ages around 1000, 900, 800, and 680, with a major peak around 600 Ma (Fig. 1c). The youngest three grains provide a weighted $^{206}\text{Pb}/^{238}\text{U}$ date of 551 ± 7 Ma (MSWD = 0.009) that we consider as the maximum deposition age for this sandstone.

6. Discussion

6.a. Radiometric age of the uppermost Brioverian beds with trace fossils

At ‘Le Lorinou’ (St-Gonlay), zircon grains from a sandstone bed associated with trace fossils yielded a maximum deposition age of 551 ± 7 Ma, whereas zircon grains from a loose sandstone sample at ‘La Lammerrais’ (St-Gonlay) gave a maximum deposition age of 540 ± 5 Ma (this study). In Crozon, the youngest U-Pb dating on zircon grains from Brioverian tuff gave an age of 543 ± 18 Ma (Guerrot *et al.* 1992), whereas another U-Pb dating on zircon grains from a sandstone gave a maximum deposition age of 546 ± 2 Ma (Ballouard *et al.* 2018). In Montfort-sur-Meu, no radiometric dating has been done so far.

The radiometric age for the base of the Cambrian is given by U-Pb dating on zircon grains from tuff in southern Oman, dated at 541.0 ± 0.13 Ma (Bowring *et al.* 2007). However,

recent U-Pb dating on zircon grains from tuff in southern Namibia constrained the age of the basal Cambrian within a 538.6–538.8 Ma interval (Linnemann *et al.* 2019). If we consider a radiometric age of *c.* 539 Ma for the base of the Cambrian, the Brioverian of Crozon could either be Ediacaran (*c.* 635–539 Ma) or younger, while the Brioverian of St-Gonlay could be Ediacaran but is suspected to be Fortunian (*c.* 539–529 Ma) or younger. Indeed, the new results of this study agree with earlier dating elsewhere (maximum deposition age of *c.* 550 Ma in Néant-sur-Yvel, Brittany, with 5 zircons grains dated at 532.1 ± 3.9 Ma; 540 ± 10 Ma in Normandy; and 540 ± 17 Ma in Mayenne; Pasteels & Doré, 1982; Guerrot *et al.* 1992; Gougeon *et al.* 2018b) and suggest an early Cambrian age for the uppermost Brioverian beds, from a radiometric standpoint (see also Guerrot *et al.* 1989, 1992; Dabard *et al.* 2021). In terms of trace fossil biostratigraphy, the matground ecology of the Brioverian is more typical of late Ediacaran assemblages (Gougeon *et al.* 2018b). Because of the differences provided by these two proxies (radiometric dating and ichnostratigraphy), definitive conclusions on the age of the uppermost Brioverian beds with trace fossils are not possible, at this point.

6.b. Critical review on Ediacaran and Cambrian planispiral trace fossils

Several trace fossils inaccurately described or suggested to be planispirals, have been reported from the Ediacaran and the Cambrian. Fedonkin (1985, 1990) erected *Planispiralichnus* Fedonkin, 1985 and *Protospiralichnus* Fedonkin, 1985 from the Fortunian Kessyuse Formation (Fm.) of northern Russia. *Planispiralichnus* is made of dense, overlapping loops (Fedonkin, 1990; Marusin & Kuper, 2020), whereas *Protospiralichnus* starts as a bounded spiral until it scribbles abundantly (Fedonkin, 1990); because of their scribbling patterns, neither of them represent spirals (Buatois *et al.* 2017). Jenkins (1995, pl. 2, fig. E) reported *cf. Protospiralichnus* from the Ediacaran Rawnsley Quartzite of southern Australia; the development of a full circle and/or a loop affiliates this trace fossil to *Circulichnis* or *Gordia* instead (see also Buatois & Mángano, 2016, fig. 2.8e).

1
2
3 329 *Multilaqueichnus* Yang & Yin, 1982 from the Cambrian Stage 3 Jiulaodong Fm. of central
4
5 330 China has overlapping loops (Yang *et al.* 1982, pl. 2, fig. 1); these trace fossils distinctly
6
7 331 scribble and are not spirals either (*contra* Mángano & Buatois, 2016, 2020). Finally, a trace
8
9 332 fossil from the Fortunian part of the Chapel Island Fm. of eastern Canada was considered a
10
11 333 spiral by Crimes & Fedonkin (1994, fig. 2i). This trace fossil has been observed in the field by
12
13 334 one of the authors (R. G.) and represents the scribbling burrow of a large infaunal deposit-
14
15 335 feeder.

16
17
18
19
20 336 In addition, non-ichnological structures from the Ediacaran and the Cambrian have
21
22 337 been mistaken for planispiral trace fossils. An important debate arose with the report of
23
24 338 Precambrian spiral fossils from the Lower Vindhyan Limestone of northeastern India (Beer,
25
26 339 1919) and from the Belt Series of northwestern USA (Walcott, 1899). Both authors suggested
27
28 340 a trace fossil origin, an opinion followed by Seilacher (1956). However, Cloud (1968)
29
30 341 suspected an algal origin, and re-evaluation of both materials confirmed that view (Walter *et*
31
32 342 *al.* 1976; Runnegar, 1991). *Arenicolites spiralis* Billings, 1872 and *Helminthoidichnites*
33
34 343 *sangshuanensis* (Du, 1986) in Yan & Liu, 1998 are certainly of similar algal affinity
35
36 344 (Hofmann, 1971; Walter *et al.* 1990; Shaowu, 1998). Furthermore, Aceñolaza (2005) reported
37
38 345 circular structures from the Cambrian Mesón Group of northwestern Argentina, and erected
39
40 346 the new ichnospecies *Spirodesmos milanai*; Minter *et al.* (2006) argued these structures were
41
42 347 formed by shrinkage cracks in matgrounds instead (cf. Pflüger, 1999; Buatois *et al.* 2013;
43
44 348 Sedorko *et al.* 2019).

45
46
47
48
49
50 349 Finally, rare horizontal spiral trace fossils have been reported from the Ediacaran and
51
52 350 the Cambrian. *Planispiralichnus rarus* Menasova, 2003 is a one-way spiral trace fossil
53
54 351 discovered in the Fortunian Khmel'nitsky Fm. of western Ukraine. The holotype is made of 3
55
56 352 whorls, with angular intervals along the course; the first two whorls are continuous, while the
57
58 353 last one is made of unconnected segments (Ivantsov *et al.* 2015, pl. 7, fig. 4a, b). This

specimen possesses the key features of a spiral trace fossil and should not be affiliated to *Planispiralichnus* as described by Fedonkin (1990). Jensen & Palacios (2016, fig. 4b) reported one-way spiral trace fossils from the Ediacaran-Fortunian Cíjara Fm. of central Spain. The photographed specimen is a continuous to discontinuous trail, with 2½ whorls and an irregular course. Carbone & Narbonne (2014, fig. 4.5) also figured an irregular one-way spiral with 1¾ whorls and a continuous course from the Fortunian part of the Ingta Fm. of northwestern Canada. Finally, Runnegar (1992, fig. 3.9) figured an irregular two-way spiral transitional with a meandering trace fossil from the Ediacaran Rawnsley Quartzite of southern Australia. Jensen (2003) considered this trace fossil to represent *Helminthorhapse* grading into *Spirorhapse*.

6.c. Macro-evolutionary profile and onshore-offshore migration

Our detailed literature review (Section 6.b above and Supplementary Material) unraveled the environmental and temporal distribution of *Spirodesmos* (Fig. 4). The Ediacaran-Fortunian is then marked by the appearance of a *Spirodesmos* pool, composed of irregular and regular forms colonizing marginal-marine to shelf environments. The Brioverian assemblage represents a key component of that pool, holding the oldest regular one-way planispirals (*Spirodesmos archimedeus*) both in marginal-marine and open shelf settings (in Montfort-sur-Meu and Crozon, respectively). During the Ediacaran and the Cambrian, deposit-feeding was the dominant feeding strategy (MacNaughton & Narbonne, 1999; Carbone & Narbonne, 2014), and early *Spirodesmos* were arguably made by epifaunal detritus-feeders and shallow-infaunal deposit-feeders. Indeed, ‘surplus stretches’ as observed in *Spirorhapse* and inferring open-burrow systems (Seilacher, 1967a, b, 1977) have not been observed in Ediacaran-Fortunian material. Moreover, Ediacaran-Fortunian *Spirodesmos* are often preserved on microbially-stabilized surfaces, which could represent the nutritive resource of their tracemaker (Carbone & Narbonne, 2014). Possible producers are

379 enteropneusts and nematodes, both suspected to first appear during the Cambrian or before
380 (Knoll & Carroll, 1999; Budd & Jensen, 2000; Maletz, 2014; Cunningham *et al.* 2017).
381 Enteropneusts produce regular horizontal spirals on the modern deep-sea floor on areas of
382 greater nutritional values, using tactile sensory systems in their head (Lemche *et al.* 1976;
383 Smith *et al.* 2005; Jones *et al.* 2013). Nematodes spiral by contracting all the muscles of one
384 side of their body (Wharton, 2004). However, spiraling in nematodes has been suggested for
385 other purposes than feeding (e.g. responses to increasing temperature, osmotic stress,
386 desiccation, and for reproduction; Huettel, 2004; Wharton, 2004).

387 [insert Figure 4]

388 Although deep-marine deposits with trace fossils have been reported both from the
389 Ediacaran (e.g. Narbonne & Hofmann, 1987; Liu *et al.* 2010) and the Cambrian (e.g.
390 Hofmann *et al.* 1994; Seilacher *et al.* 2005), planispirals are consistently absent. However,
391 planispirals are common through the rest of the Phanerozoic in the deep-sea, and *Spirodesmos*
392 forms a conspicuous Ordovician–Recent deep-marine trend (Fig. 4 and Supplementary
393 Material). Deep-marine seafloors are characterized by an absence of light, high hydrostatic
394 pressure, oxygen and temperature fluctuations, and low nutrient content (Sanders & Hessler,
395 1969; Gage & Tyler, 1991, pp. 9–29; Rex & Etter, 2010, pp. 1–49). These stressful conditions
396 play an important role on animal fitness and their physiology (e.g. Childress & Thuesen,
397 1992; Yancey *et al.* 2004; van der Grient & Rogers, 2015). However, with the increased
398 **competition** for space and food on early Cambrian shelves (Orr, 2001), planispiral
399 tracemakers may have adapted their metabolisms to the deep-sea. An onshore-offshore
400 migration in *Spirodesmos* is then suggested from the Ediacaran-Fortunian to the Ordovician,
401 similarly to the migration observed in graphoglyptids (Crimes & Anderson, 1985; Crimes *et*
402 *al.* 1992; Crimes & Fedonkin, 1994; Orr, 2001; Uchman, 2003). The existence of an onshore-
403 offshore migration is also reinforced by the presence of an important gap (*c.* 230 Ma) between

the Ediacaran-Fortunian *Spirodesmos* pool, and the next shallow-marine *Spirodesmos* report from the Permian Vryheid Fm. of eastern South Africa (Mason *et al.* 1983; Fig. 4).

7. Conclusion

The age of the uppermost Brioverian deposits of central Brittany, northwestern France, is a long-standing question. Here, two U-Pb detrital zircon grain dating on sandstone samples collected in St-Gonlay gave maximum depositional ages of 551 ± 7 Ma and 540 ± 5 Ma. Although an Ediacaran age for the uppermost Brioverian beds cannot be discarded, a Fortunian age is suggested in this study, following previous dating in Brittany, Normandy, and Mayenne. However, the intervals of error of the radiometric dating and trace fossil biostratigraphy do not allow definitive conclusions.

A unique assemblage of irregular and regular, one-way planispiral trace fossils of *Spirodesmos* affinity has been recovered from the uppermost Brioverian beds in Crozon, Montfort-sur-Meu, and St-Gonlay. Planispiral trace fossils are unusual in the Ediacaran and the Cambrian, and an in-depth literature review revealed that the Brioverian assemblage belonged to an Ediacaran-Fortunian, marginal-marine to shelf *Spirodesmos* pool. Ediacaran-Fortunian *Spirodesmos* were arguably made by detritus- or deposit-feeders, possibly related to enteropneusts or nematodes. However, by the Ordovician, *Spirodesmos* became conspicuous mostly in the deep-marine realm, underscoring an onshore-offshore migration similar to what has been reported in graphoglyptids.

Acknowledgements

This manuscript is a follow-up of a poster presented at the International Meeting on the Ediacaran System and the Ediacaran-Cambrian Transition (IMECT) that took place in Guadalupe, Spain, in October 2019. Discussions and feedbacks from L. Buatois, P. Crimes, G. Mángano, V. Marusin, and M. Paz are kindly acknowledged. We also thank: M. Ferguson

for double-checking the English writing; D. Gendry and S. Regnault for granting access to the museum of the Geological Institute of the University of Rennes 1 and the Museum of Natural History of Nantes, respectively; N. Hallot for the rock crushing; E. Hanson for sharing her photographs of the trace fossil from Crozon; X. Le Coz for the rock sawing and preparation of thin sections; Y. Lepagnot for mineral separations; F. Polette and L. Guillois for their assistance during U-Pb dating; and the outcrops' owners for granting access to their private properties. The manuscript benefited from insightful reviews by A. Uchman and an anonymous reviewer, as well as editor S. Jensen. The work of A. L. has been partially supported by the 'Fondazione Banco di Sardegna' and by the 'Regione Autonoma della Sardegna' (grant numbers F74I19000960007, J81G17000110002). This publication is a contribution to the VIBRIO project of the INSU InterrVie program, and benefitted from a financial support from the 'Observatoire des Sciences de l'Univers de Rennes' (OSUR). We have a special thought for our colleague M.-P. Dabard who passed away too soon.

Declaration of Interest

None.

References

- Aceñolaza GF** (2005) *Spirodesmos milanai* n. isp.: a shallow-water spiral trace fossil from the Cambrian of the eastern Cordillera, northwest Argentina. *Ichnos* **12**, 59–63.
- Andrée K** (1920) Über einige fossile Problematika. I. Ein Problematikum aus dem Paläozoikum von Battenberg an der Eder und des dasselbe beherbergende Gestein. *Neues Jahrbuch für Mineralogie, Geologie und Paläontologie* **1**, 55–88.
- Auvray B, Mace J, Vidal P and Van der Voo R** (1980) Rb-Sr dating of the Plouézec volcanics, N Brittany: implications for the age of red beds ('Séries rouges') in the northern Armorican Massif. *Journal of the Geological Society* **137**, 207–10.

- 452 **Ballèvre M, Bosse V, Dabard M-P, Ducassou C, Fourcade S, Paquette J-L, Peucat J-J**
 453 **and Pitra P** (2013) Histoire géologique du Massif Armoricaïn: **a**ctualité de la recherche.
 454 *Bulletin de la Société Géologique et Minéralogique de Bretagne* **10-11**, 5–96.
- 455 **Ballouard C, Poujol M and Zeh A** (2018) Multiple crust reworking in the French Armorican
 456 Variscan belt: implication for the genesis of uranium-fertile leucogranites. *International*
 457 *Journal of Earth Sciences* **107**, 2317–36.
- 458 **Beer EJ** (1919) Note on a spiral impression on Lower Vindhyan Limestone. *Records of the*
 459 *Geological Survey of India* **50**, 139.
- 460 **Billings E** (1872) On some fossils from the primordial rocks of Newfoundland. *Canadian*
 461 *Naturalist and Quarterly Journal of Science* **6**, 465–79.
- 462 **Bonjour JL and Odin GS** (1989) Recherche sur les volcanoclastites des Séries Rouges
 463 Initiales en presqu'île de Crozon: **p**remier âge radiométrique de l'Arénig. *Géologie de la*
 464 *France* **4**, 3–7.
- 465 **Bonjour JL, Peucat JJ, Chauvel JJ, Paris F and Cornichet J** (1988) U-Pb zircon dating of
 466 the early Paleozoic (Arenigian) transgression in Western Brittany (France): **a** new constraint
 467 for the lower Paleozoic time-scale. *Chemical Geology (Isotope Geoscience section)* **72**, 329–
 468 36.
- 469 **Bottjer DJ, Hagadorn JW and Dornbos SQ** (2000) The Cambrian substrate revolution.
 470 *GSA Today* **10(9)**, 1–7.
- 471 **Bowring SA, Grotzinger JP, Condon DJ, Ramezani J, Newall MJ and Allen PA** (2007)
 472 Geochronologic constraints on the chronostratigraphic framework of the Neoproterozoic Huqf
 473 Supergroup, Sultanate of Oman. *American Journal of Science* **307**, 1097–145.

- 474 **Boyle RA, Dahl TW, Bjerrum CJ and Canfield DE** (2018) Bioturbation and directionality
475 in Earth's carbon isotope record across the Neoproterozoic–Cambrian transition. *Geobiology*
476 **16**, 252–78.
- 477 **Brasier M, Cowie J and Taylor M** (1994) Decision on the Precambrian-Cambrian boundary
478 stratotype. *Episodes* **17**, 3–8.
- 479 **Buatois LA and Mángano MG** (2016) Ediacaran ecosystems and the dawn of animals. In
480 *The trace-fossil record of major evolutionary events, Volume 1: Precambrian and Paleozoic*
481 (eds MG Mángano and LA Buatois), pp. 27–72. Dordrecht: Springer.
- 482 **Buatois LA, Netto RG, Mángano MG and Carmona NB** (2013) Global deglaciation and
483 the re-appearance of microbial matground-dominated ecosystems in the late Paleozoic of
484 Gondwana. *Geobiology* **11**, 307–17.
- 485 **Buatois LA, Wisshak M, Wilson MA and Mángano MG** (2017) Categories of architectural
486 designs in trace fossils: a measure of ichnodisparity. *Earth-Science Reviews* **164**, 102–81.
- 487 **Budd GE and Jensen S** (2000) A critical reappraisal of the fossil record of the bilaterian
488 phyla. *Biological Reviews* **75**, 253–95.
- 489 **Canfield DE and Farquhar J** (2009) Animal evolution, bioturbation, and the sulfate
490 concentration of the oceans. *Proceedings of the National Academy of Sciences* **106**, 8123–7.
- 491 **Carbone C and Narbonne GM** (2014) When life got smart: the evolution of behavioral
492 complexity through the Ediacaran and Early Cambrian of NW Canada. *Journal of*
493 *Paleontology* **88**, 309–30.
- 494 **Cayeux L** (1894) Sur la présence de restes de Foraminifères dans les terrains précambriens de
495 Bretagne. *Annales de la Société Géologique du Nord* **22**, 116–9.

- 496 **Chantraine J, Chauvel J-J, Dupret L, Gatinot F, Icart J-C, Le Corre C, Rabu D, Sauvan**
 497 **P and Villey M** (1982) Inventaire lithologique et structural du Briovérien (Protérozoïque
 498 supérieur) de la Bretagne centrale et du Bocage normand. *Bulletin du BRGM* **1**, 3–17.
- 499 **Chantraine J, Egal E, Thiéblemont D, Le Goff E, Guerrot C, Ballèvre M and Guennoc P**
 500 (2001) The Cadomian active margin (North Armorican Massif, France): a segment of the
 501 North Atlantic Panafrican belt. *Tectonophysics* **331**, 1–18.
- 502 **Chauvel JJ and Mansuy C** (1981) Micropaléontologie du Protérozoïque du Massif
 503 Armoricaïn (France). *Precambrian Research* **15**, 25–42.
- 504 **Chauvel JJ and Schopf JW** (1978) Late Precambrian microfossils from Brioverian cherts
 505 and limestones of Brittany and Normandy, France. *Nature* **275**, 640–2.
- 506 **Childress JJ and Thuesen EV** (1992) Metabolic potential of deep-sea animals: regional and
 507 global scales. In *Deep-sea food chains and the global carbon cycle* (eds GT Rowe and V
 508 Pariente), pp. 217–36. **Dordrecht: Springer.**
- 509 **Cloud PE** (1968) Pre-metazoan evolution and the origins of the Metazoa. In *Evolution and*
 510 *environment* (ed. ET Drake), pp. 1–72. **New Haven: Yale University Press.**
- 511 **Cogné J** (1959) Données nouvelles sur l'Antécambrien dans l'Ouest de la France : Pentévrien
 512 et Briovérien en baie de Saint-Brieuc (Côtes-du-Nord). *Bulletin de la Société Géologique de*
 513 *France* **7**, 112–8.
- 514 **Crimes TP** (1987) Trace fossils and correlation of late Precambrian and early Cambrian
 515 strata. *Geological Magazine* **124**, 97–119.
- 516 **Crimes TP** (1992a) Changes in the trace fossil biota across the Proterozoic-Phanerozoic
 517 boundary. *Journal of the Geological Society, London* **149**, 637–46.

- 1
2
3 518 **Crimes TP** (1992*b*) The record of trace fossils across the Proterozoic-Cambrian boundary. In
4
5 519 *Origin and early evolution of the Metazoa* (eds JH Lipps and PW Signor), pp. 177–99. New
6
7 York: Plenum Press.
8
9
10 521 **Crimes TP** (1994) The period of early evolutionary failure and the dawn of evolutionary
11
12 success: the record of biotic changes across the Precambrian-Cambrian boundary. In *The*
13 522 *palaeobiology of trace fossils* (ed. SK Donovan), pp. 105–33. Chichester: John Wiley & Sons.
14
15
16
17
18 524 **Crimes TP and Anderson MM** (1985) Trace fossils from Late Precambrian-Early Cambrian
19
20 strata of southeastern Newfoundland (Canada): temporal and environmental implications.
21 525
22 *Journal of Paleontology* **59**, 310–43.
23
24
25
26 527 **Crimes TP and Crossley JD** (1991) A diverse ichnofauna from Silurian flysch of the
27
28 Aberystwyth Grits Formation, Wales. *Geological Journal* **26**, 27–64.
29
30
31 529 **Crimes TP and Fedonkin MA** (1994) Evolution and dispersal of deepsea traces. *Palaios* **9**,
32
33 530 74–83.
34
35
36 531 **Crimes TP, Garcia Hidalgo JG and Poire DG** (1992) Trace fossils from Arenig flysch
37
38 sediments of Eire and their bearing on the early colonisation of the deep seas. *Ichnos* **2**, 61–
39 532
40 77.
41
42
43
44 534 **Crimes TP, Marcos A and Perez-Estaun A** (1974) Upper Ordovician turbidites in western
45
46 Asturias: a facies analysis with particular reference to vertical and lateral variations.
47 535
48 *Palaeogeography, Palaeoclimatology, Palaeoecology* **15**, 169–84.
49 536
50
51 537 **Crimes TP and McCall GJH** (1995) A diverse ichnofauna from Eocene-Miocene rocks of
52
53 the Makran Range (SE Iran). *Ichnos* **3**, 231–58.
54 538
55
56
57 539 **Cunningham JA, Liu AG, Bengtson S and Donoghue PC** (2017) The origin of animals:
58
59 540 can molecular clocks and the fossil record be reconciled? *BioEssays* **39**, 1–12.
60

- 541 **D’Lemos RS, Strachan RA and Topley CG** (1990) The Cadomian orogeny in the North
542 Armorican Massif: a brief review. In *The Cadomian Orogeny* (eds RS D’Lemos, R Strachan
543 and CG Topley), pp. 3–12. Geological Society, London, Special Publication No. 51.
- 544 **Dabard MP** (1990) Lower Brioverian formations (Upper Proterozoic) of the Armorican
545 Massif (France) : geodynamic evolution of source areas revealed by sandstone petrography
546 and geochemistry. *Sedimentary Geology* **69**, 45–58.
- 547 **Dabard MP** (2000) Petrogenesis of graphitic cherts in the Armorican segment of the
548 Cadomian orogenic belt (NW France). *Sedimentology* **47**, 787–800.
- 549 **Dabard MP and Loi A** (1998) Environnement de dépôt des formations à phanites
550 interstratifiés du Protérozoïque supérieur armoricain (France) : conséquences sur la genèse
551 des phanites. *Comptes Rendus de l’Académie des Sciences de Paris* **326**, 763–9.
- 552 **Dabard MP, Loi A, Pavanetto P, Meloni MA, Hauser N, Matteini M and Funedda A**
553 (2021) Provenance of Ediacaran-Ordovician sediments of the Medio Armorican Domain,
554 Brittany, West France: constraints from U/Pb detrital zircon and Sm–Nd isotope data.
555 *Gondwana Research* **90**, 63–76.
- 556 **Dabard MP, Loi A and Peucat JJ** (1996) Zircon typology combined with Sm–Nd whole-
557 rock isotope analysis to study Brioverian sediments from the Armorican Massif. *Sedimentary*
558 *Geology* **101**, 243–60.
- 559 **Dabard MP and Simon B** (2011) Discordance des Séries Rouges Initiales sur le socle
560 briovérien : exemple de la carrière des Landes. *Bulletin de la Société Géologique et*
561 *Minéralogique de Bretagne* **8**, 33–44.
- 562 **Dalrymple RW** (2010) Tidal depositional systems. In *Facies Models 4* (eds NP James and
563 RW Dalrymple), pp. 201–231. The Geological Association of Canada.

- 564 **Dangeard L, Doré F and Juignet P** (1961) Le Briovérien supérieur de Basse Normandie
565 (étage de la Laize), série à turbidites, a tous les caractères d'un flysch. *Revue de Géographie*
566 *Physique et de Géologie Dynamique* **4**, 251–9.
- 567 **Deflandre G** (1955) *Paleocryptidium* n. g. *cayeuxi* n. sp., microorganismes incertae sedis des
568 phtanites briovériens bretons. *Comptes Rendus Sommaires de la Société Géologique de*
569 *France* **9-10**, 182–5.
- 570 **Denis E** (1988) Les sédiments briovériens (Protérozoïque supérieur) de Bretagne
571 septentrionale et occidentale : nature, mise en place et évolution. *Mémoires et Documents du*
572 *Centre Armoricaïn d'Etude Structurale des Socles* **18**, pp. 263.
- 573 **Denis E and Dabard MP** (1988) Sandstone petrography and geochemistry of late
574 Proterozoic sediments of the Armorican Massif (France) - a key to basin development during
575 the Cadomian Orogeny. *Precambrian Research* **42**, 189–206.
- 576 **Dickinson WR and Gehrels GE** (2009) Use of U-Pb ages of detrital zircons to infer
577 maximum depositional ages of strata: a test against a Colorado Plateau Mesozoic database.
578 *Earth Planetary Science Letters* **288**, 115–25.
- 579 **Dissler E, Doré F, Dupret L, Gresselin F and Le Gall J** (1988) L'évolution géodynamique
580 cadomienne du Nord-Est du Massif armoricain. *Bulletin de la Société Géologique de France*
581 **4**, 801–14.
- 582 **Fedonkin MA** (1985) Paleoichnology of Vendian metazoa. In *The Vendian System 1:*
583 *Historic-Geological and Palaeontological Basis* (eds BS Sokolov and AB Ivanovskiy), pp.
584 112–6. Moscow: Nauka.
- 585 **Fedonkin MA** (1990) Paleoichnology of Vendian metazoa. In *The Vendian System 1:*
586 *Paleontology* (eds BS Sokolov and AB Iwanoski), pp. 132–341. Berlin: Springer.

- 587 **Gage JD and Tyler PA** (1991) *Deep-sea biology: a natural history of organisms at the deep-*
 588 *sea floor*. Cambridge, UK: Cambridge University Press, 504 pp.
- 589 **Geinitz HB** (1867) Die organischen Ueberreste im Dachschiefer von Wurzbach bei
 590 Lobenstein. In *Ueber ein Aequivalent der takonischen Schiefer Nordamerika's in Deutschland*
 591 *und dessen geologische Stellung* (eds HB Geinitz and KT Liebe), pp. 1–24. Dresden: Druck
 592 von E. Blochmann & Sohn.
- 593 **Gehling JG** (1999) Microbial mats in terminal Proterozoic siliciclastics: Ediacaran death
 594 masks. *Palaios* **14**, 40–57.
- 595 **Gougeon RC, Mángano MG, Buatois LA, Narbonne GM and Laing BA** (2018a) Early
 596 Cambrian origin of the shelf sediment mixed layer. *Nature Communications* **9**, 1909.
- 597 **Gougeon R, Néraudeau D, Dabard MP, Pierson-Wickmann AC, Polette F, Poujol M.**
 598 **and Saint-Martin JP** (2018b) Trace Fossils from the Brioverian (Ediacaran–Fortunian) in
 599 Brittany (NW France). *Ichnos* **25**, 11–24.
- 600 **Gougeon R, Néraudeau D, Poujol M and Loi A** (2019) Loops, circles, spirals and the
 601 appearance of guided behaviors from the Ediacaran-Cambrian of Brittany, NW France.
 602 *Estudios Geológicos* **75**, p002, 11–3.
- 603 **Graindor M-J** (1957) Le Briovérien dans le Nord-Est du Massif Armoricaín. *Mémoires pour*
 604 *servir à l'explication de la Carte Géologique détaillée de la France*, 211 pp.
- 605 **Guerrot C, Calvez JY, Bonjour JL, Chantaine J, Chauvel JJ, Dupret L and Rabu D**
 606 (1992) Le Briovérien de Bretagne centrale et occidentale : nouvelles données radiométriques.
 607 *Comptes Rendus de l'Académie des Sciences de Paris* **315**, 1741–6.

- 608 **Guerrot C, Peucat JJ and Dupret L** (1989) Données nouvelles sur l'âge du système
609 briovérien (Protérozoïque supérieur) dans le Nord du Massif armoricain. *Comptes Rendus de*
610 *l'Académie des Sciences de Paris* **308**, 89–92.
- 611 **Häntzschel W** (1975) *Treatise on invertebrate paleontology. Part W, Miscellanea,*
612 *supplement 1: Trace Fossils and Problematica.* Boulder: The Geological Society of America,
613 Inc, and The University of Kansas.
- 614 **Heer O** (1876) *Flora Fossilis Helvetiae. Die Vorweltliche Flora der Schweiz.* Zürich: Verlag
615 von J. Wurster & Comp.
- 616 **Hofmann HJ** (1971) Precambrian fossils, pseudofossils and problematica in Canada.
617 *Geological Survey of Canada, Bulletin* **189**, 1–146.
- 618 **Hofmann HJ, Cecile MP and Lane LS** (1994) New occurrences of *Oldhamia* and other
619 trace fossils in the Cambrian of the Yukon and Ellesmere Island, arctic Canada. *Canadian*
620 *Journal of Earth Sciences* **31**, 767–82.
- 621 **Horn M** (1989) Die Lebensspur *Spirodesmos* im Unterkarbon des Östlichen Rheinischen
622 Schiefergebirges. *Bulletin de la Société Belge de Géologie* **98**, 385–91.
- 623 **Huckriede R** (1952) Eine spiralförmige Lebensspur aus dem Kulmkieselschiefer von
624 Biedenkopf an der Lahn (*Spirodesmos archimedeus* n. sp.). *Paläontologische Zeitschrift* **26**,
625 175–80.
- 626 **Huettel RN** (2004) Reproductive behaviour. In *Nematode Behaviour* (eds R Gaugler and AL
627 Bilgrami), pp. 127–149. Wallingford: CABI Publishing.
- 628 **Ivantsov AY, Gritsenko VP, Paliy VM, Velikanov VA, Konstantinenko LI, Menasova**
629 **AS, Fedonkin MA, Zakrevskaya MA and Serezhnikova EA** (2015) *Upper Vendian*
630 *macrofossils of Eastern Europe. Middle Dniester area and Volhynia.* PIN: Moscow, 144 pp.

- 631 **Jenkins RJ** (1995) The problems and potential of using animal fossils and trace fossils in
632 terminal Proterozoic biostratigraphy. *Precambrian Research* **73**, 51–69.
- 633 **Jensen S** (2003) The Proterozoic and earliest Cambrian trace fossil record; patterns, problems
634 and perspectives. *Integrative and Comparative Biology* **43**, 219–28.
- 635 **Jensen S and Palacios T** (2016) The Ediacaran-Cambrian trace fossil record in the Central
636 Iberian Zone, Iberian Peninsula. *Comunicações Geológicas* **103** (Especial I), 83–92.
- 637 **Jones DOB, Alt CHS, Priede IG, Reid WDK, Wigham BD, Billett DSM, Gebruk AV,**
638 **Rogacheva A and Gooday AJ** (2013) Deep-sea surface-dwelling enteropneusts from the
639 Mid-Atlantic Ridge: their ecology, distribution and mode of life. *Deep Sea Research II* **98**,
640 374–87.
- 641 **Kitchell JA, Kitchell JF, Johnson GL and Hunkins KL** (1978) Abyssal traces and
642 megafauna: comparison of productivity, diversity and density in the Arctic and Antarctic.
643 *Paleobiology* **4**, 171–80.
- 644 **Knoll AH and Carroll SB** (1999) Early animal evolution: emerging views from comparative
645 biology and geology. *Science* **284**, 2129–37.
- 646 **Książkiewicz M** (1977) Trace fossils in the flysch of the Polish Carpathians. *Palaeontologia*
647 *Polonica* **36**, 1–208.
- 648 **Le Corre C, Auvray B, Ballèvre M and Robardet M** (1991) Le Massif Armoricaïn.
649 *Sciences Géologiques, Bulletin* **44**, 31–103.
- 650 **Lebesconte P** (1886) Constitution générale du Massif Breton. *Bulletin de la Société*
651 *Géologique de France, 3ème série* **17**, 776–91.
- 652 **Lemche H, Hansen B, Madsen FJ, Tendal OS and Wolff T** (1976) Hadal life as analyzed
653 from photographs. *Videnskabelige Meddelelser dansk naturhistorisk Forening* **139**, 263–336.

- 654 **Linnemann U, Ovtcharova M, Schaltegger U, Gärtner A, Hautmann M, Geyer G,**
655 **Vickers-Rich P, Rich T, Plessen B, Hofmann M, Zieger J, Krause R, Kriesfeld L and**
656 **Smith J** (2019) New high-resolution age data from the Ediacaran–Cambrian boundary
657 indicate rapid, ecologically driven onset of the Cambrian explosion. *Terra Nova* **31**, 49–58.
- 658 **Liu AG, McIlroy D and Brasier MD** (2010) First evidence for locomotion in the Ediacara
659 biota from the 565 Ma Mistaken Point Formation, Newfoundland. *Geology* **38**, 123–6.
- 660 **Logan GA, Hayes JM, Hieshima GB and Summons RE** (1995) Terminal Proterozoic
661 reorganization of biogeochemical cycles. *Nature* **376**, 53–6.
- 662 **MacNaughton RB and Narbonne GM** (1999) Evolution and ecology of Neoproterozoic-
663 Lower Cambrian trace fossils, NW Canada. *Palaios* **14**, 97–115.
- 664 **Maletz J** (2014) Hemichordata (Pterobranchia, Enteropneusta) and the fossil record.
665 *Palaeogeography, Palaeoclimatology, Palaeoecology* **398**, 16–27.
- 666 **Malusà MG, Carter A, Limoncelli M, Villa IM and Garzanti E** (2013) Bias in detrital
667 zircon geochronology and thermochronometry. *Chemical Geology* **359**, 90–107.
- 668 **Mángano MG and Buatois LA** (2014) Decoupling of body-plan diversification and
669 ecological structuring during the Ediacaran-Cambrian transition: evolutionary and
670 geobiological feedbacks. *Proceedings of the Royal Society B: Biological Sciences* **281**,
671 20140038.
- 672 **Mángano MG and Buatois LA** (2016) The Cambrian Explosion. In *The trace-fossil record*
673 *of major evolutionary events, Volume 1: Precambrian and Paleozoic* (eds MG Mángano and
674 LA Buatois), pp. 73–126. Dordrecht: Springer.
- 675 **Mángano MG and Buatois LA** (2020) The rise and early evolution of animals: where do we
676 stand from a trace-fossil perspective? *Interface Focus* **10**, 20190103.

- 677 **Manzotti P, Poujol M and Ballèvre M** (2015) Detrital zircon geochronology in blueschist-
 678 facies meta-conglomerates from the Western Alps: implications for the late Carboniferous to
 679 early Permian palaeogeography. *International Journal of Earth Sciences* **104**, 703–31.
- 680 **Mansuy C and Vidal G** (1983) Late Proterozoic Brioverian microfossils from France:
 681 taxonomic affinity and implications of plankton productivity. *Nature* **302**, 606–7.
- 682 **Marusin VV and Kuper KE** (2020) Complex tunnel systems of early Fortunian macroscopic
 683 endobenthos in the Ediacaran-Cambrian transitional strata of the Olenek Uplift (NE Siberian
 684 Platform). *Precambrian Research* **340**, 105627.
- 685 **Mason TR, Stanistreet IG and Tavener-Smith R** (1983) Spiral trace fossils from the
 686 Permian Ecca Group of Zululand. *Lethaia* **16**, 241–7.
- 687 **McMahon WJ, Davies NS and Went DJ** (2017) Negligible microbial matground influence
 688 on pre-vegetation river functioning: evidence from the Ediacaran-Lower Cambrian Series
 689 Rouge, France. *Precambrian Research* **292**, 13–34.
- 690 **Menasova AS** (2003) New representatives of the Vendian biota from localities of Podolia.
 691 *Zbirnik naukovikh prats' IGN: Teoretichni ta prikladni aspekti suchasnoi biostratigrafii fan*
 692 *erozoyu Ukraine*, 139–42.
- 693 **Meysman FJ, Middelburg JJ and Heip CH** (2006) Bioturbation: a fresh look at Darwin's
 694 last idea. *Trends in Ecology & Evolution* **21**, 688–95.
- 695 **Minter NJ and Braddy SJ** (2009) Ichnology of an Early Permian intertidal flat: the Robledo
 696 Mountains Formation of southern New Mexico, USA. *Special Papers in Paleontology* **82**, 1–
 697 107.
- 698 **Minter NJ, Buatois LA, Lucas SG, Braddy SJ and Smith JA** (2006) Spiral-shaped
 699 graphoglyptids from an Early Permian intertidal flat. *Geology* **34**, 1057–60.

- 700 **Narbonne GM and Hofmann HJ** (1987) Ediacaran biota of the Wernecke Mountains,
701 Yukon, Canada. *Palaeontology* **30**, 647–76.
- 702 **Narbonne GM, Myrow PM, Landing E and Anderson MM** (1987) A candidate stratotype
703 for the Precambrian–Cambrian boundary, Fortune head, Burin Peninsula, southeastern
704 Newfoundland. *Canadian Journal of Earth Sciences* **24**, 1277–93.
- 705 **Néraudeau D, Dabard M-P, El Albani A, Gougeon R, Mazurier A, Pierson-Wickmann**
706 **A-C, Poujol M, Saint Martin J-P and Saint Martin S** (2019) First evidence of Ediacaran–
707 Fortunian elliptical body fossils in the Brioverian series of Brittany, NW France. *Lethaia* **51**,
708 513–22.
- 709 **Néraudeau D, Gougeon R, Dabard M-P and Poujol M** (2016) Les traces de vie de la limite
710 Ediacarien-Cambrien dans le Massif armoricain. *Géochroniques* **140**, 26–8.
- 711 **Nio SD and Yang CS** (1991) Diagnostic attributes of clastic tidal deposits: a review. In
712 *Clastic Tidal Sedimentology* (eds DG Smith, GE Reinson, BA Zaitlin and RA Rahmani), pp.
713 3–28. Canadian Society of Petroleum Geologists, Memoir 16.
- 714 **Noffke N, Gerdes G, Klenke T and Krumbein WE** (2001) Microbially induced
715 sedimentary structures: a new category within the classification of primary sedimentary
716 structures. *Journal of Sedimentary Research* **71**, 649–56.
- 717 **Orr PJ** (2001) Colonization of the deep-marine environment during the early Phanerozoic:
718 the ichnofaunal record. *Geological Journal* **36**, 265–78.
- 719 **Pasteels P and Doré F** (1982) Age of the Vire-Carolles granite. In *Numerical Dating in*
720 *Stratigraphy* (ed GS Odin), pp. 784–91. Chichester: John Wiley & Sons.
- 721 **Pflüger F** (1999) Matground structures and redox facies. *Palaaios* **14**, 25–39.

- 722 **Rabu D, Chantraine J, Chauvel JJ, Denis E, Balé P and Bardy P** (1990) The Brioverian
 723 (Upper Proterozoic) and the Cadomian orogeny in the Armorican Massif. In *The Cadomian*
 724 *Orogeny* (eds RS D'Lemos, RA Strachan and CG Topley), pp. 81–94. Geological Society,
 725 London, Special Publication No. 51.
- 726 **Rex MA and Etter RJ** (2010) *Deep-sea biodiversity: pattern and scale*. Cambridge, MA:
 727 Harvard University Press, 368 pp.
- 728 **Runnegar B** (1991) Precambrian oxygen levels estimated from the biochemistry and
 729 physiology of early eukaryotes. *Global and Planetary Change* **5**, 97–111.
- 730 **Runnegar BN** (1992) Evolution of the earliest animals. In *Major events in the history of life*
 731 (ed. JW Schopf), pp. 65–93. Boston: Jones and Bartlett Publishers.
- 732 **Sacco F** (1888) Note di paleoicnologia Italiana. *Atti della Società Italiana di Scienze Naturali*
 733 **31**, 151–92.
- 734 **Sanders HL and Hessler RR** (1969) Ecology of the deep-sea benthos. *Science* **163**, 1419–
 735 24.
- 736 **Sedorko D, Netto RG and Horodyski RS** (2019) Tracking Silurian-Devonian events and
 737 paleobathymetric curves by ichnologic and taphonomic analyzes in the southwestern
 738 Gondwana. *Global and Planetary Change* **179**, 43–56.
- 739 **Seilacher A** (1956) Der Beginn des Kambriums als biologische Wende. *Neues Jahrbuch für*
 740 *Geologie und Paläontologie, Abhandlungen* **103**, 155–80.
- 741 **Seilacher A** (1967a) Vorzeitliche Mäanderspuren. In *Die Strassen der Tiere* (ed H. Hediger),
 742 pp. 294–306. Wiesbaden: Vieweg+Teubner Verlag.
- 743 **Seilacher A** (1967b) Fossil behavior. *Scientific American* **217**, 72–83.

- 744 **Seilacher A** (1974) Flysch trace fossils: evolution of behavioural diversity in the deep-sea.
745 *Neues Jahrbuch für Geologie und Paläontologie, Monatshefte*, 233–45.
- 746 **Seilacher A** (1977) Pattern analysis of *Paleodictyon* and related trace fossils. In *Trace fossils*
747 2 (eds **TP Crimes and JC Harper**), pp. 289–334. **Liverpool: Seel House Press**.
- 748 **Seilacher A** (1986) Evolution of behavior as expressed in marine trace fossils. In *Evolution of*
749 *animal behavior: paleontological and field approaches* (eds JA Kitchell and MH Nitecki), pp.
750 62–87. **New York: Oxford University Press**.
- 751 **Seilacher A, Buatois LA and Mángano MG** (2005) Trace fossils in the Ediacaran-Cambrian
752 transition: behavioral diversification, ecological turnover and environmental shift.
753 *Palaeogeography, Palaeoclimatology, Palaeoecology* **227**, 323–56.
- 754 **Seilacher A and Pflüger F** (1994) From biomats to benthic agriculture: a biohistoric
755 revolution. In *Biostabilization of sediments* (eds WE Krumbein, DM Paterson and LJ Stal),
756 pp. 97–105. Bibliotheks und Informationssystem der Universität Oldenburg.
- 757 **Shaowu N** (1998) Confirmation of the genus *Grypania* (megascopic alga) in Gaoyuzhuang
758 Formation (1434Ma) in Jixian (Tianjin) and its significance. *Progress in Precambrian*
759 *Research* **21**, 36–46.
- 760 **Smith KL, Holland ND and Ruhl HA** (2005) Enteropneust production of spiral fecal trails
761 on the deep-sea floor observed with time-lapse photography. *Deep Sea Research Part I:*
762 *Oceanographic Research Papers* **52**, 1228–40.
- 763 **Stepanek J and Geyer G** (1989) Spurenfossilien aus dem Kulm (Unterkarbon) des
764 Frankenwaldes. *Beringeria* **1**, 1–55.
- 765 **Tessier B, Archer AW, Lanier WP and Feldman HR** (1995) Comparison of ancient tidal
766 rhythmites (Carboniferous of Kansas and Indiana, USA) with modern analogues (the Bay of

- Mont-Saint-Michel, France). In *Tidal Signatures in Modern and Ancient Sediments* (eds BW Flemming and A Bartholomä), pp. 259–71. Special Publication Number 24 of the International Association of Sedimentologists.
- Trautmann F, Paris F and Carn A** (1999) *Notice explicative, Carte géologique de France (1/50 000), feuille Rennes (317)*. Orléans: BRGM, 85 pp.
- Uchman A** (1998) Taxonomy and ethology of flysch trace fossils: revision of the Marian Książkiewicz collection and studies of complementary material. *Annales Societatis Geologorum Poloniae* **68**, 105–218.
- Uchman A** (2003) Trends in diversity, frequency and complexity of graphoglyptid trace fossils: evolutionary and palaeoenvironmental aspects. *Palaeogeography, Palaeoclimatology, Palaeoecology* **192**, 123–42.
- Van der Grient JM and Rogers AD** (2015) Body size versus depth: regional and taxonomical variation in deep-sea meio- and macrofaunal organisms. In *Advances in marine biology* (ed. BE Curry), pp. 71–108. Cambridge, MA: Academic Press Vol. 71.
- Vermeesch P** (2018) IsoplotR: a free and open toolbox for geochronology. *Geoscience Frontiers* **9**, 1479–93.
- Walcott CD** (1899) Pre-Cambrian fossiliferous formations. *Bulletin of the Geological Society of America* **10**, 199–244.
- Walter MR, Du R and Horodyski RJ** (1990) Coiled carbonaceous megafossils from the Middle Proterozoic of Jixian (Tianjin) and Montana. *American Journal of Science* **290**, 133–48.

- 788 **Walter MR, Oehler JH and Oehler DZ** (1976) Megascopic algae 1300 million years old
789 from the Belt Supergroup, Montana: a reinterpretation of Walcott's *Helminthoidichnites*.
790 *Journal of Paleontology* **50**, 872–81.
- 791 **Went DJ** (2017) Alluvial fan, braided river and shallow-marine turbidity current deposits in
792 the Port Lazo and Roche Jagu formations, Northern Brittany: relationships to andesite
793 emplacements and implications for age of the Plourivo-Plouézec Group. *Geological Magazine*
794 **154**, 1037–60.
- 795 **Wharton DA** (2004) Survival strategies. In *Nematode Behaviour* (eds R Gaugler and AL
796 Bilgrami), pp. 371–99. Wallingford: CABI Publishing.
- 797 **Xia B, Lu H, Xiong B, He Y and Hu B** (1987) *Spirodesmos kaihuaensis* in the upper
798 Ordovician flysch in the Kaihua County, west part of Zhejiang province. *Acta*
799 *Sedimentologica Sinica* **5**, 73–9.
- 800 **Yan Y and Liu Z** (1998) Does *Sangshuania* represent eukaryotic algae or trace fossils? *Acta*
801 *Micropalaeontologica Sinica* **15**, 101–10.
- 802 **Yancey PH, Rhea MD, Kemp K and Bailey DM** (2004) Trimethylamine oxide, betaine and
803 other osmolytes in deep-sea animals: depth trends and effects on enzymes under hydrostatic
804 pressure. *Cellular and Molecular Biology* **50**, 371–6.
- 805 **Yang Z, Yin J and He T** (1982) Early Cambrian trace fossils from the Emei-Ganluo region,
806 Sichuan, and other localities. *Geological Review* **28**, 291–8.
- 807 **Zapletal J and Pek I** (1971) Nález spirálních bioglyfů v kulmu Nížkého Jeseníku. *Časopis*
808 *pro Mineralogii a Geologii* **16**, 285–9.

Figure 1. Geological map of northwestern France, and new U-Pb dating. (a) Location of the Brioverian deposits in northwestern France. (b) Close-up showing the Brioverian deposits, and the three localities with planispiral trace fossils. NASZ = North-Armorican Shear Zone; SASZ = South-Armorican Shear Zone. (c) Kernel Density Estimation diagrams for ‘La Lammerais’ and ‘Le Lorinou’ samples.

Figure 2. Terminology of planispirals. (a) An irregular one-way spiral. (b) A regular one-way spiral. (c) A regular two-way spiral. (d) A bounded spiral. See text for further explanations.

Figure 3. *Spirodesmos* isp. and *Spirodesmos archimedeus* from the uppermost Brioverian beds of Brittany. (a) *Spirodesmos* isp. (irregular one-way spiral trace fossil) from ‘Le Bois-du-Buisson’. (b, c) *Spirodesmos archimedeus* (regular one-way spiral trace fossils) from ‘Les Grippeaux’ (b) and ‘La Plage-du-Goulien’ (c). Scale bars are 1 cm across.

Figure 4. Macro-evolutionary profile of *Spirodesmos* comparable to the Brioverian material, with emphasis on the Ediacaran and the Cambrian (colored diagrams). Positions suggested for the Brioverian material are emphasized by diagrams with dashed lines. Brioverian *Spirodesmos* belonged to an Ediacaran-Fortunian, marginal-marine to shelf pool. A *Spirodesmos* onshore-offshore migration is suggested, from the Ediacaran-Fortunian to the Ordovician. See text for further explanations.

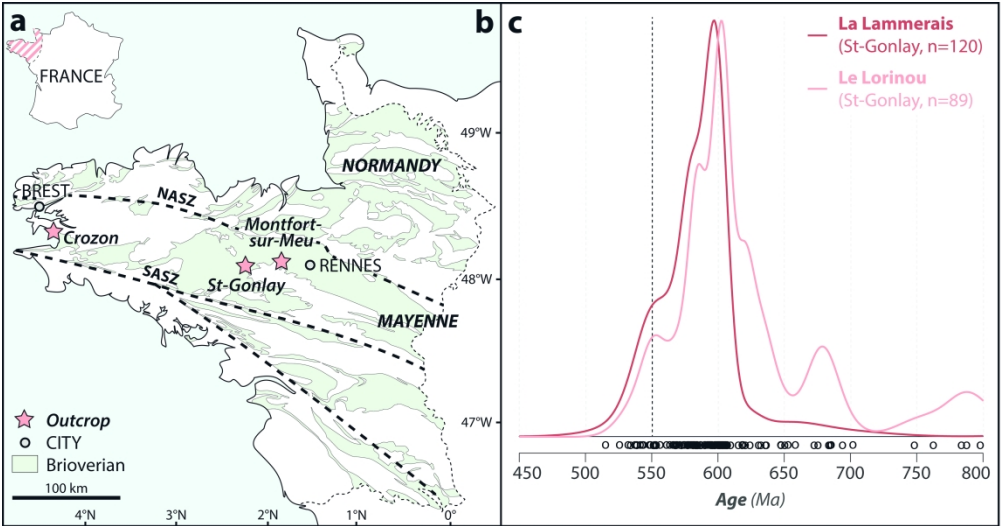


Figure 1. Geological map of northwestern France, and new U-Pb dating. (a) Location of the Brioverian deposits in northwestern France. (b) Close-up showing the Brioverian deposits, and the three localities with planispiral trace fossils. NASZ = North-Armorican Shear Zone; SASZ = South-Armorican Shear Zone. (c) Kernel Density Estimation diagrams for 'La Lammerais' and 'Le Lorinou' samples.

168x88mm (600 x 600 DPI)

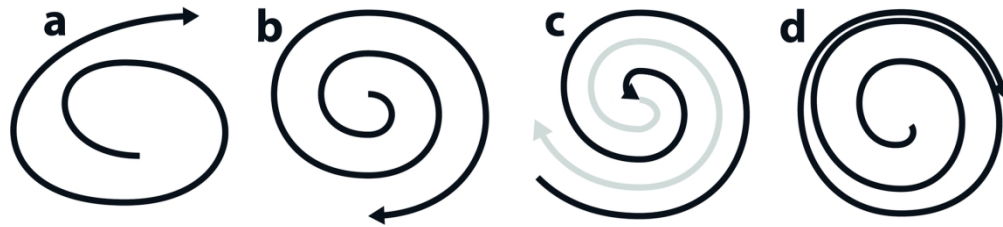


Figure 2. Terminology of planispirals. (a) An irregular one-way spiral. (b) A regular one-way spiral. (c) A regular two-way spiral. (d) A bounded spiral. See text for further explanations.

80x18mm (600 x 600 DPI)

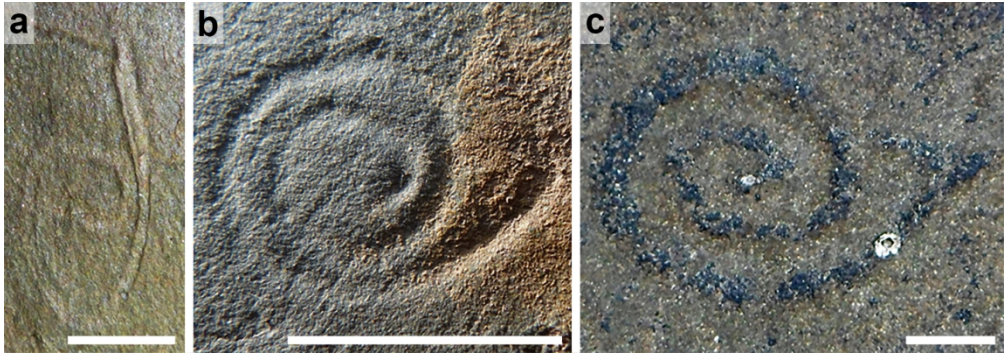


Figure 3. *Spirodesmos* isp. and *Spirodesmos archimedeus* from the uppermost Brioverian beds of Brittany. (a) *Spirodesmos* isp. (irregular one-way spiral trace fossil) from 'Le Bois-du-Buisson'. (b, c) *Spirodesmos archimedeus* (regular one-way spiral trace fossils) from 'Les Grippeaux' (b) and 'La Plage-du-Goulien' (c). Scale bars are 1 cm across.

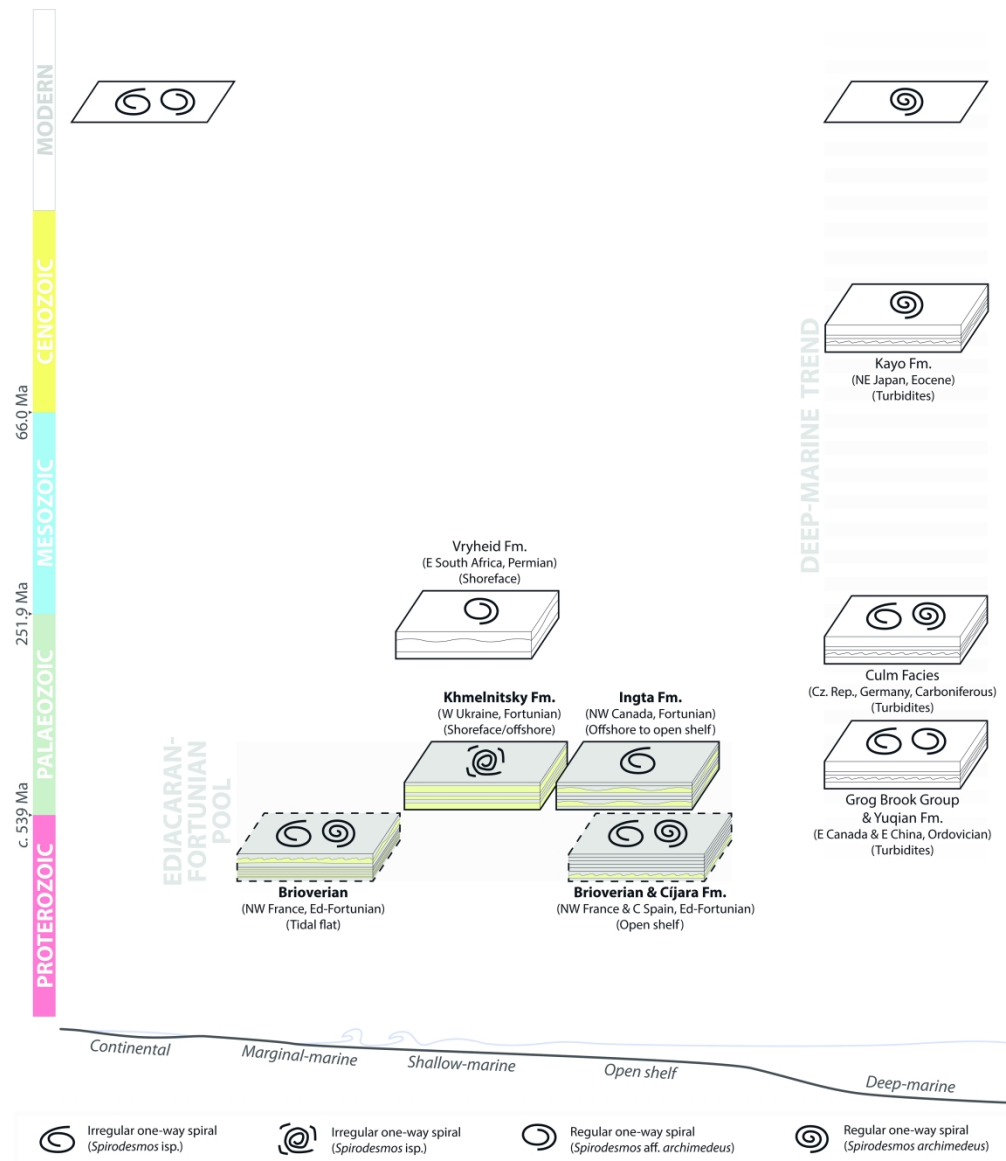


Figure 4. Macro-evolutionary profile of *Spirodesmos* comparable to the Brioverian material, with emphasis on the Ediacaran and the Cambrian (colored diagrams). Positions suggested for the Brioverian material are emphasized by diagrams with dashed lines. Brioverian *Spirodesmos* belonged to an Ediacaran-Fortunian, marginal-marine to shelf pool. A *Spirodesmos* onshore-offshore migration is suggested, from the Ediacaran-Fortunian to the Ordovician. See text for further explanations.

168x195mm (600 x 600 DPI)

1
2
3
4
5
6
7
8
9
10
11
12
13
14
15
16
17
18
19
20
21
22
23
24
25
26
27
28
29
30
31
32
33
34
35
36
37
38
39
40
41
42
43
44
45
46
47
48
49
50
51
52
53
54
55
56
57
58
59
60

Geological Magazine

New insights on the early evolution of horizontal spiral trace fossils and the age of the
Brioverian (Ediacaran-Cambrian) in Brittany, NW France

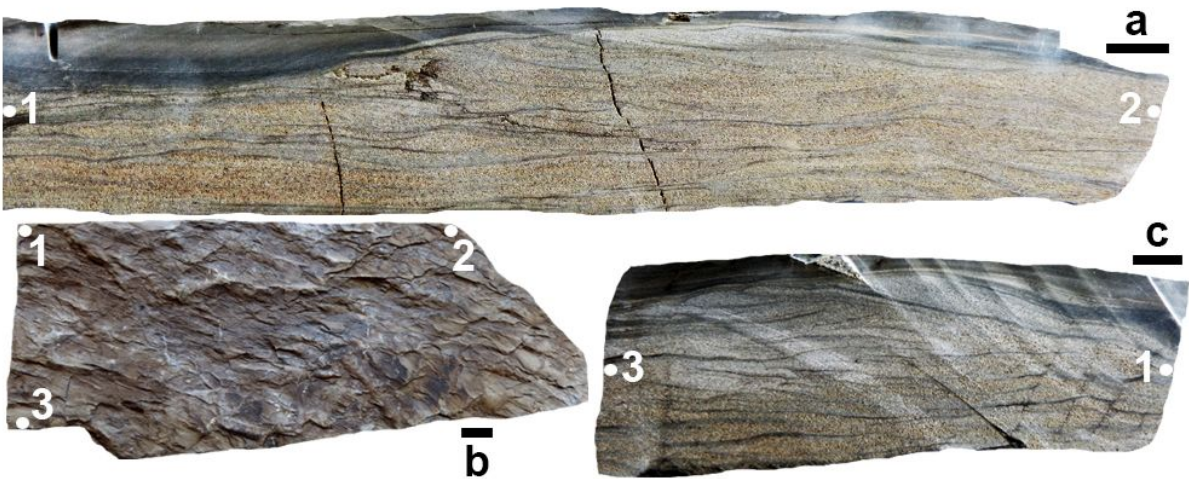
Romain Gougeon,, Didier Néraudeau, Alfredo Loi and Marc Poujol

Supplementary Material

For Peer Review

Laboratory & Sample Preparation	
Laboratory name	GeOHeLiS Analytical Platform (OSUR, Univ. Rennes 1)
Sample type/mineral	Zircon
Sample preparation	Conventional mineral separation, 1 inch resin mount, 1micron polish to finish
Imaging	RELION CL instrument, Olympus Microscope BX51WI, Leica Color Camera DFC 420C
Laser ablation system	
Make, Model & type	ESI NWR193UC, Excimer
Ablation cell	ESI NWR TwoVol2
Laser wavelength	193 nm
Pulse width	< 5 ns
Fluence	7.4 J/cm ²
Repetition rate	3Hz
Spot size	20 µm
Sampling mode / pattern	Single spot
Carrier gas	100% He, Ar make-up gas and N ₂ (3 ml/mn) combined using in-house smoothing device
Background collection	20 seconds
Ablation duration	60 seconds
Wash-out delay	15 seconds
Cell carrier gas flow (He)	0.75 l/min
ICP-MS Instrument	
Make, Model & type	Agilent 7700x, Q-ICP-MS
Sample introduction	Via conventional tubing
RF power	1350W
Sampler, skimmer cones	Ni
Extraction lenses	X type
Make-up gas flow (Ar)	0.80 l/min
Detection system	Single collector secondary electron multiplier
Data acquisition protocol	Time-resolved analysis
Scanning mode	Peak hopping, one point per peak
Detector mode	Pulse counting, dead time correction applied, and analog mode when signal intensity > ~ 10 ⁶ cps
Masses measured	²⁰⁴ (Hg + Pb), ²⁰⁶ Pb, ²⁰⁷ Pb, ²⁰⁸ Pb, ²³² Th, ²³⁸ U
Integration time / peak	10–30 ms (²⁰⁷ Pb)
Sensitivity / Efficiency	22000 cps/ppm Pb (50µm, 10Hz)
Data Processing	
Gas blank	20 seconds on-peak
Calibration strategy	GJ1 zircon standard used as primary reference material, Plešovice used as secondary reference material (quality control)
Common-Pb correction	No common-Pb correction.
Reference Material info	GJ1 (Jackson <i>et al.</i> 2004), Plešovice (Sláma <i>et al.</i> 2008)
Data processing package	Glitter (Van Achterbergh <i>et al.</i> 2001)
Uncertainty level and propagation	Ages are quoted at 2 sigma absolute, propagation is by quadratic addition according to Horstwood <i>et al.</i> (2016). Reproducibility and age uncertainty of reference material are propagated.
Quality control/ Validation	Plešovice: concordia age = 336.9± 2.0 Ma (N=36; MSWD=1.7)

Supplementary Table S1. Operating conditions for the LA-ICP-MS equipment.



Supplementary Figure 1. A fine-grained sandstone sample from Chanteloup under three different views (a, c: side views; b: surface view) showing abundant and discontinuous mud-draper (i.e. flaser-lamination; cf. Nichols, 2009, fig. 4.37). The numbers are marker points for a three-dimensional understanding of the sample. Scale bars are 1 cm across.

Supplementary Discussion

1. Review on Phanerozoic planispirals

The Ordovician is marked by the first record of uncontroversial *Spirorhaphe* in turbidites from the Grog Brook Group in eastern Canada (Pickerill, 1980, fig. 2b). This specimen is a regular two-way spiral with $1\frac{1}{2}$ whorls; also associated is a regular *Spirodesmos* with $1\frac{1}{4}$ whorls (Pickerill, 1980, fig. 2d). Fillion & Pickerill (1990, pl. 17, figs 17, 18) described ‘scribbling grazing traces’ from the Ordovician Redmans Fm. in eastern Canada; few of these specimens represent distinctive one-way spirals with $1-1\frac{1}{2}$ whorls (i.e. *Spirodesmos* affinity; Fillion & Pickerill, 1990, pl. 17, fig. 18). In eastern China, the Ordovician Yuqian Fm. contains an assemblage of trace fossils with *Spirodesmos kaihuaensis* deposited in deep-water turbidites (Xia *et al.* 1987; Jin & Li, 1998); these are irregular one-way spirals made of 3–5 whorls (Xia *et al.* 1987, pl. 1, fig. 1). Crimes *et al.* (1974, fig. 2) mentioned *Spirophycus* in turbidites from the Ordovician Agüeira Fm. of northwestern Spain, but only a sketch representing an irregular one-way spiral with $1\frac{1}{4}$ whorls is provided. Interestingly, a spiral burrow was reported from the Ordovician Kermeur Fm. in northwestern France (Vidal *et al.* 2011, fig. 4b), close to the locality where a Brioverian spiral was also found (Fig. 2c). Deposited in proximal settings, the irregular one-way spiral burrow has a variable width, develops $1\frac{1}{2}$ whorls and has a fill clearly different from the host rock. Its closest relatives are *Spirophycus* as described by Chamberlain & Clark (1973, pl. 2, fig. 1) from the Carboniferous of western USA, and by Mikuláš (1993, pl. 2, fig. 1) from the Ordovician of northern Czech Republic. Finally, *Spirodesmos spiralis* from the Ordovician Železný Brod Phyllites of northern Czech Republic (Chlupáč, 1997, pl. 6, fig. 2) is deformed (possibly due to metamorphism), and its ichnotaxonomic affiliation is problematic.

After the Ordovician, abundant *Spirophycus* (e.g. Sacco, 1888; Chamberlain & Clark, 1973; Crimes, 1977; Książkiewicz, 1977; Crimes & McCall, 1995; Buatois *et al.* 2001;

Uchman, 2007) and *Spirorhappe* (e.g. Abel, 1935, pp. 291, 292; Macsotay, 1967; Książkiewicz, 1977; McCann & Pickerill, 1988; Crimes & McCall, 1995; Uchman, 2001; Monaco & Trecci, 2014) were reported from the deep-sea as part of the *Nereites* ichnofacies. Most of the record of post-Ordovician deep-marine *Spirodesmos* is coming from the Carboniferous Culm Facies of Germany and Czech Republic, represented by *S. archimedeus* (Huckriede, 1952; Zapletal & Pek, 1971; Horn, 1989; Pek & Zapletal, 1990), *S. interruptus* (Andrée, 1920; Horn, 1989), and *S. spiralis* (Geinitz, 1867; Stepanek & Geyer, 1989; Pek & Zapletal, 1990). Other occurrences of *Spirodesmos* in the Phanerozoic are: (1) from the Triassic Al Ayn Fm. of Oman, with only ½ whorl preserved which is problematic (Wetzel *et al.* 2007); and (2) from the Eocene Kayo Fm. of northeastern Japan, with 3½ whorls preserved (Fukuda & Hayasaka, 1978).

Continental occurrences are scarce and only comprise a large *Spirodesmos interruptus* from the Carboniferous Mansfield Fm. of northeastern USA (Archer & Maples, 1984, fig. 5b). This irregular one-way spiral has 1½ whorls, and is made of segments of variable length; Rindsberg & Kopaska-Merkel (2005) argued for a *Treptichnus* affinity instead. Kim *et al.* (2002, fig. 5h) recorded a partially preserved *Spirodesmos* isp. from the Cretaceous Hasandong Fm. of southern Korea; with the absence of at least one fully developed whorl, this continental occurrence remains dubious.

In marginal-marine settings, Minter *et al.* (2006) and Minter & Braddy (2009) reported cf. *Spirorhappe azteca* from the Permian Robledo Mountains Fm. of southern USA. These are regular one-way spirals with closely spaced, millimetric whorls (up to 19 whorls; Minter *et al.* 2006, fig. 1).

In shallow-marine environments, *Spirodesmos archimedeus* is reported from the Permian Vryheid Fm. of eastern South-Africa (Mason *et al.* 1983). These regular one-way spirals, with 1¼–1½ whorls, are reminiscent of the Ordovician ‘scribbling grazing traces’ of

Fillion & Pickerill (1990, pl. 17, fig. 18). *Macaronichnus segregatis spiriformis* Bromley, Milàn, Uchman & Hansen, 2009 has been reported from the Cretaceous Horseshoe Canyon Fm. of western Canada (Pemberton *et al.* 2001). Although these planispirals are regular with multiple whorls, they differ from other spiral trace fossils by their light-colored infill and their thin, dark mantle (Pemberton *et al.* 2001, fig. 104). Finally, Gierlowski-Kordesch & Ernst (1987) reported a unique assemblage of graphoglyptids with *Spirorhappe* deposited under storm conditions in the Cretaceous Nangurukuru Fm. of southeastern Tanzania (see also Ernst & Zanders, 1993; Nicholas *et al.* 2006).

2. Review on modern planispirals

From continental settings, Schäfer (1965) reported one-way, tightly coiled spirals from mud banks of the Rhine river in Germany. Although Schäfer (1965) suspected grazing gastropod tracemakers, he failed in observing an animal in action. MacNaughton (2003) found one-way spirals with either irregular tight whorls or regular whorls increasing space outward (i.e. logarithmic spirals) from a lake beach in eastern Canada. MacNaughton (2003) suspected a small infaunal arthropod to be the originator. Muñiz Guinea *et al.* (2014) described regular one-way spirals from a wet orange grove in southwestern Spain. These traces were made by an infaunal fly larvae, and are continuous (incipient *Spirodesmos*) or displaying lateral projections (combination of incipient *Spirodesmos* and *Treptichnus*). Finally, a one-way spiral trace was reported by Metz (1987, fig. 4) from a puddle in eastern USA, made by an epifaunal ground beetle larva.

In tidal settings, *Paraonis* polychaete worms are well-known for constructing infaunal, tightly-coiled regular one-way spirals (Röder, 1971; Schäfer, 1972, p. 296; Risk & Tunnicliffe, 1978; Bromley, 1996, pp. 105-108; Minter *et al.* 2006; Lehane & Ekdale, 2013). The burrow system is made of multiple horizontal spirals occupying different vertical levels, and connected by vertical shafts (Gripp, 1927; Röder, 1971; Gingras *et al.* 1999). In addition,

incipient *Macaronichnus segregatis spiriformis* are made by *Ophelia* and *Thoracophelia* polychaete worms in beach sands (Pemberton *et al.* 2001; Bromley *et al.* 2009; Quiroz *et al.* 2019).

Owing to the development of submarine photography in the middle of the 20th century (Ewing *et al.* 1946; Emery, 1952), the deep ocean exposed two categories of spiral traces: (1) one-way spirals (incipient *Spirodesmos*), and (2) two-way spirals (incipient *Spirorhaphé*). Reports of one-way spirals are prolific in the literature (e.g. Bourne & Heezen, 1965; Hülsemann, 1966; Jacobs *et al.* 1970, pp. 391, 445; Lemche *et al.* 1976; Foell & Pawson, 1986; Holland *et al.* 2005; Durden *et al.* 2019); they are made by acorn worms, a type of giant enteropneust (Bourne & Heezen, 1965; Holland *et al.* 2005), and can be extremely abundant below 2500 m (Heezen & Hollister, 1971, pp. 176, 177; Kitchell *et al.* 1978*a, b*; Kitchell, 1979; Bell *et al.* 2013). Two-way spiral traces are more rarely photographed on the deep-sea floor (Ewing & Davis, 1967; Ekdale & Berger, 1978; Berger *et al.* 1979; Ekdale, 1980; Ekdale *et al.* 1984), and their tracemaker has never been identified.

Additional references

Abel O (1935) *Vorzeitliche lebensspuren*. Jena: Gustav Fischer, 644 pp.

Archer AW and Maples CG (1984) Trace-fossil distribution across a marine-to-nonmarine gradient in the Pennsylvanian of southwestern Indiana. *Journal of Paleontology* **58**, 448–66.

Bell JB, Jones DO and Alt CH (2013) Lebensspuren of the bathyal mid-Atlantic ridge. *Deep Sea Research II* **98**, 341–51.

Berger WH, Ekdale AA and Bryant PP (1979) Selective preservation of burrows in deep-sea carbonates. *Marine Geology* **32**, 205–30.

Bourne DW and Heezen BC (1965) A wandering enteropneust from the abyssal Pacific, and the distribution of “spiral” tracks on the sea floor. *Science* **150**, 60–3.

Bromley R (1996) *Trace fossils biology, taphonomy and applications*. Second edition. London: Chapman & Hall, 361 pp.

Bromley RG, Milàn J, Uchman A and Hansen KS (2009) Rheotactic *Macaronichnus*, and human and cattle trackways in Holocene beachrock, Greece: reconstruction of paleoshoreline orientation. *Ichnos* **16**, 103–17.

Buatois LA, Mángano MG and Sylvester Z (2001) A diverse deep-marine ichnofauna from the Eocene Tarcau sandstone of the Eastern Carpathians, Romania. *Ichnos* **8**, 23–62.

Chamberlain CK and Clark DL (1973) Trace fossils and conodonts as evidence for deep-water deposits in the Oquirrh Basin of central Utah. *Journal of Paleontology* **47**, 663–82.

Chlupáč I (1997) Palaeozoic ichnofossils in phyllites near Železný Brod, northern Bohemia. *Journal of the Czech Geological Society* **42**, 75–86.

Crimes TP (1977) Trace fossils of an Eocene deep-sea fan, northern Spain. In *Trace fossils 2* (eds TP Crimes and JC Harper), pp. 71–90. Liverpool: Seel House Press.

Durden JM, Bett BJ, Huffard CL, Pebody C, Ruhl HA and Smith KL (2019) Response of deep-sea deposit-feeders to detrital inputs: a comparison of two abyssal time-series sites. *Deep Sea Research II*, <https://doi.org/10.1016/j.dsr2.2019.104677>.

Ekdale AA (1980) Graphoglyptid burrows in modern deep-sea sediment. *Science* **207**, 304–6.

Ekdale AA and Berger WH (1978) Deep-sea ichnofacies: modern organism traces on and in pelagic carbonates of the western equatorial Pacific. *Palaeogeography, Palaeoclimatology, Palaeoecology* **23**, 263–78.

Ekdale AA, Muller LN and Novak MT (1984) Quantitative ichnology of modern pelagic deposits in the abyssal Atlantic. *Palaeogeography, Palaeoclimatology, Palaeoecology* **45**, 189–223.

Emery KO (1952) Submarine photography with the benthograph. *The Scientific Monthly* **75**, 3–11.

Ernst G and Zander J (1993) Stratigraphy, facies development, and trace fossils of the Upper Cretaceous of southern Tanzania (Kilwa District). In *Geology and Mineral Resources of Somalia and Surrounding Regions* (eds E Abbate, M Sagri and FP Sassi), pp. 259–78. Firenze: Relazioni e Monografie Agrarie Subtropicali e Tropicali, Nuova Serie, 113.

Ewing M and Davis RA (1967) Lebensspuren photographed on the ocean floor. In *Deep-sea photography* (ed. JB Hersey), pp. 259–94. Baltimore: The John Hopkins Press.

Ewing M, Vine A and Worzel JL (1946) Photography of the ocean bottom. *Journal of the Optical Society of America* **36**, 307–21.

Fillion D and Pickerill RK (1990) Ichnology of the Upper Cambrian? to Lower Ordovician Bell Island and Wabana groups of eastern Newfoundland, Canada. *Palaeontographica Canadiana* **7**, 1–119.

Foell EJ and Pawson DL (1986) Photographs of invertebrate megafauna from abyssal depths of the north-eastern equatorial Pacific Ocean. *The Ohio Journal of Science* **86**, 61–8.

Fukuda Y and Hayasaka S (1978) Trace fossils from the Eocene Kayo Formation in Okinawa-Shima, Ryukyu Islands, Japan. *Reports of the Faculty of Science, Kagoshima University: Earth Sciences and Biology* **11**, 13–25.

Gierlowski-Kordesch E and Ernst G (1987) A flysch trace fossil assemblage from the Upper Cretaceous shelf of Tanzania. In *Current Research in African Earth Sciences* (eds G Matheis and H Schandelmeier), pp. 217–21. Rotterdam: Balkema.

Gingras MK, Pemberton SG, Saunders T and Clifton HE (1999) The ichnology of modern and Pleistocene brackish-water deposits at Willapa Bay, Washington: variability in estuarine settings. *Palaios* **14**, 352–74.

Gripp K (1927) Über einen ‘geführte Mäander’ erzeugenden Bewohner des Ostsee-Litorals. *Senckenbergiana* **9**, 93–9.

Heezen BC and Hollister CD (1971) *The face of the deep*. New York: Oxford University Press, 659 pp.

Holland ND, Clague DA, Gordon DP, Gebruk A, Pawson DL and Vecchione M (2005) ‘Lophenteropneust’ hypothesis refuted by collection and photos of new deep-sea hemichordates. *Nature* **434**, 374–6.

Horstwood MSA, Košler J, Gehrels G, Jackson SE, McLean NM, Paton C, Pearson NJ, Sircombe K, Sylvester P, Vermeesch P, Bowring JF, Condon DJ and Schoene B (2016) Community-derived standards for LA-ICP-MS U-(Th-)Pb geochronology - uncertainty propagation, age interpretation and data reporting. *Geostandards and Geoanalytical Research* **40**, 311–32.

Hülsemann J (1966) Spiralfährten und “geführte Mäander” auf dem Meeresboden. *Natur und Museum* **96**, 449–55.

Jackson SE, Pearson NJ, Griffin WL and Belousova EA (2004) The application of laser ablation-inductively coupled plasma-mass spectrometry to in situ U-Pb zircon geochronology. *Chemical Geology* **211**, 47–69.

- Jacobs SS, Bruchhausen PM and Bauer EB** (1970) *Eltanin reports, Cruises 32–36, 1968*. Hydrographic Stations Bottom Photographs, Current Measurements, Lamont-Doherty Geological Observatory of Columbia Univ. New York: Palisades, 460 pp.
- Jin H and Li Y** (1998) Environmental significance of a *Spirodesmos* ichnofossil assemblage from the upper Ordovician Yuqian Formation in the western Zhejiang province, China. *Scientia Geologica Sinica* **33**, 282–9.
- Kim JY, Kim K-S and Pickerill R** (2002) Cretaceous nonmarine trace fossils from the Hasandong and Jinju Formations of the Namhae Area, Kyongsangnamdo, southeast Korea. *Ichnos* **9**, 41–60.
- Kitchell JA** (1979) Deep-sea foraging pathways: an analysis of randomness and resource exploitation. *Paleobiology* **5**, 107–25.
- Kitchell JA, Kitchell JF, Clark DL and Dangeard L** (1978b) Deep-sea foraging behavior: its bathymetric potential in the fossil record. *Science* **200**, 1289–91.
- Lehane JR and Ekdale AA** (2013) Pitfalls, traps, and webs in ichnology: traces and trace fossils of an understudied behavioral strategy. *Palaeogeography, Palaeoclimatology, Palaeoecology* **375**, 59–69.
- MacNaughton RB** (2003) Planispiral burrows from a Recent lacustrine beach, Gander Lake, Newfoundland. *The Canadian Field-Naturalist* **117**, 577–81.
- Macsotay O** (1967) Huellas problematicas y su valor paleoecologico en Venezuela. *Geos* **16**, 7–79.
- McCann T and Pickerill RK** (1988) Flysch trace fossils from the Cretaceous Kodiak Formation of Alaska. *Journal of Paleontology* **62**, 330–48.
- Metz R** (1987) Insect traces from nonmarine ephemeral puddles. *Boreas* **16**, 189–95.

- Mikuláš R** (1993) New information on trace fossils of the Early Ordovician of Prague Basin (Barrandian area, Czech Republic). *Journal of the Czech Geological Society* **38**, 171–82.
- Monaco P and Trecci T** (2014) Ichnocoenoses in the Macigno turbidite basin system, Lower Miocene, Trasimeno (Umbrian Apennines, Italy). *Italian Journal of Geosciences* **133**, 116–30.
- Muñiz Guinea F, Mángano MG, Buatois LA, Podeniene V, Gamez Vintaned JA and Mayoral Alfaro E** (2014) Compound biogenic structures resulting from ontogenetic variation: an example from a modern dipteran. *Spanish Journal of Palaeontology* **29**, 83–94.
- Nicholas CJ, Pearson PN, Bown PR, Jones TD, Huber BT, Karega A, Lees JA, McMillan IK, O'Halloran A, Singano JM and Wade BS** (2006) Stratigraphy and sedimentology of the Upper Cretaceous to Paleogene Kilwa Group, southern coastal Tanzania. *Journal of African Earth Sciences* **45**, 431–66.
- Nichols G** (2009) *Sedimentology and Stratigraphy*. Second edition. Chichester: John Wiley & Sons, 419 pp.
- Pek I and Zapletal J** (1990) Progress report: the importance of ichnology in geologic studies of the eastern Bohemian Massif (lower Carboniferous), Czechoslovakia. *Ichnos* **1**, 147–9.
- Pemberton SG, Spila M, Pulham AJ, Saunders T, MacEachern JA, Robbins D and Sinclair IK** (2001) Ichnology and sedimentology of shallow to marginal marine systems. *Geological Association of Canada, Short Course Notes* **15**, 1–343.
- Pickerill RK** (1980) Phanerozoic flysch trace fossil diversity - observations based on an Ordovician flysch ichnofauna from the Aroostook–Matapedia Carbonate Belt of northern New Brunswick. *Canadian Journal of Earth Sciences* **17**, 1259–70.

Quiroz LI, Buatois LA, Seike K, Mángano MG, Jaramillo C and Sellers AJ (2019) The search for an elusive worm in the tropics, the past as a key to the present, and reverse uniformitarianism. *Scientific Reports* **9**, 18402.

Rindsberg AK and Kopaska-Merkel DC (2005) *Treptichnus* and *Arenicolites* from the Steven C. Minkin Paleozoic footprint site (Langsettian, Alabama, USA). In *Pennsylvanian Footprints in the Black Warrior Basin of Alabama* (eds RJ Buta, AK Rindsberg and DC Kopaska-Merkel), pp. 121–41. Birmingham: Alabama Paleontological Society Monograph No. 1.

Risk MJ and Tunnicliffe VJ (1978) Intertidal spiral burrows: *Paraonis fulgens* and *Spiophanes wigleyi* in the Minas Basin, Bay of Fundy. *Journal of Sedimentary Research* **48**, 1287–92.

Röder H (1971) Gangsysteme von *Paraonis fulgens* Levinsen 1883 (Polychaeta) in ökologischer, ethologischer und aktuopalaontologischer Sicht. *Senckenbergiana Maritima* **3**, 3–51.

Schäfer W (1965) Aktuopalaontologische Beobachtungen. 4. Spiralfährten und “geführte Mäander”. *Natur und Museum* **95**, 83–90.

Schäfer W (1972) *Ecology and palaeoecology of marine environments*. Edinburgh: Oliver & Boyd, 568 pp.

Sláma J, Kosler J, Condon DJ, Crowley JL, Gerdes A, Hanchar JM, Horstwood MSA, Morris GA, Nasdala L, Norberg N, Schaltegger U, Schoene B, Tubrett MN and Whitehouse MJ (2008) Plesovice zircon - a new natural reference material for U-Pb and Hf isotopic microanalysis. *Chemical Geology* **249**, 1–35.

1
2
3 **Uchman A** (2001) Eocene flysch trace fossils from the Hecho Group of the Pyrenees,
4 northern Spain. *Beringeria* **28**, 3–41.
5
6
7

8 **Uchman A** (2007) Deep-sea trace fossils from the mixed carbonate-siliciclastic flysch of the
9 Monte Antola Formation (Late Campanian-Maastrichtian), North Apennines, Italy.
10
11
12 *Cretaceous Research* **28**, 980–1004.
13
14
15

16 **Vidal M, Loi A, Dabard MP and Botquelen A** (2011) A Palaeozoic open shelf benthic
17 assemblage in a protected marine environment. *Palaeogeography, Palaeoclimatology,*
18 *Palaeoecology* **306**, 27–40.
19
20
21
22

23 **Wetzel A, Blechschmidt I, Uchman A and Matter A** (2007) A highly diverse ichnofauna in
24 Late Triassic deep-sea fan deposits of Oman. *Palaios* **22**, 567–76.
25
26
27
28
29
30
31
32
33
34
35
36
37
38
39
40
41
42
43
44
45
46
47
48
49
50
51
52
53
54
55
56
57
58
59
60

							Isoto
	Analysis_#	Pb ppm	Uppm	Th ppm	Th/U	Pb207/U235	PropErr2sigAbs.
	Carrière de Lammerais:						
	S-230517a-01	49	534	48	0.09	0.947	0.012
	S-230517a-02	16	164	60	0.37	0.779	0.010
	S-230517a-03	65	151	152	1.00	6.876	0.087
	S-230517a-04	27	278	103	0.37	0.770	0.010
	S-230517a-05	11	111	53	0.48	0.770	0.011
	S-230517a-06	29	300	130	0.43	0.752	0.010
	S-230517a-07	27	333	18	0.05	0.748	0.010
	S-230517a-08	23	259	75	0.29	0.727	0.010
	S-230517a-09	11	114	38	0.33	0.819	0.011
	S-230517a-10	61	565	278	0.49	0.838	0.011
	S-230517a-11	20	194	83	0.43	0.787	0.011
	S-230517a-12	18	178	68	0.38	0.839	0.012
	S-230517a-13	34	316	201	0.64	0.791	0.010
	S-230517a-14	18	186	92	0.49	0.760	0.010
	S-230517a-15	45	504	153	0.30	0.728	0.010
	S-230517a-16	30	294	106	0.36	0.810	0.011
	S-230517a-17	20	205	63	0.31	0.792	0.011
	S-230517a-18	19	189	57	0.30	0.805	0.011
	S-230517a-19	18	190	42	0.22	0.811	0.011
	S-230517a-20	23	235	69	0.29	0.816	0.012
	S-230517a-21	17	179	64	0.36	0.756	0.011
	S-230517a-22	31	333	134	0.40	0.749	0.010
	S-230517a-23	18	196	56	0.29	0.786	0.012
	S-230517a-24	18	193	63	0.33	0.785	0.011
	S-230517b-01	36	369	294	0.80	0.826	0.011
	S-230517b-02	26	293	105	0.36	0.738	0.010
	S-230517b-03	18	178	64	0.36	0.793	0.011
	S-230517b-04	33	336	101	0.30	0.809	0.011
	S-230517b-05	44	451	118	0.26	0.812	0.011
	S-230517b-06	27	275	83	0.30	0.806	0.011
	S-230517b-07	25	254	77	0.30	0.851	0.011
	S-230517b-08	39	383	229	0.60	0.772	0.010
	S-230517b-09	25	263	89	0.34	0.759	0.010
	S-230517b-10	36	380	192	0.50	0.743	0.010
	S-230517b-11	25	261	54	0.21	0.837	0.011
	S-230517b-12	41	446	87	0.20	0.807	0.011
	S-230517b-13	21	177	94	0.53	0.948	0.013
	S-230517b-15	72	720	289	0.40	0.792	0.010
	S-230517b-16	20	192	94	0.49	0.793	0.011
	S-230517b-17	40	431	156	0.36	0.751	0.010
	S-230517b-18	22	265	48	0.18	0.704	0.009
	S-230517b-19	27	311	54	0.17	0.722	0.010
	S-230517b-21	60	410	117	0.29	1.439	0.019

1							
2	S-230517b-22	29	313	102	0.33	0.764	0.010
3	S-230517b-23	28	284	115	0.40	0.766	0.010
4	S-230517b-24	24	281	80	0.29	0.710	0.010
5	S-230517c-01	48	516	128	0.25	0.781	0.010
6	S-230517c-02	66	813	17	0.02	0.756	0.010
7	S-230517c-03	29	248	88	0.35	1.008	0.013
8	S-230517c-04	39	386	165	0.43	0.812	0.011
9	S-230517c-05	407	4195	486	0.16	1.278	0.046
10	S-230517c-06	38	379	129	0.34	0.813	0.011
11	S-230517c-07	35	355	125	0.35	0.810	0.011
12	S-230517c-08	18	187	42	0.23	0.800	0.011
13	S-230517c-09	28	308	85	0.27	0.772	0.010
14	S-230517c-10	24	264	35	0.13	0.771	0.010
15	S-230517c-11	29	331	94	0.29	0.712	0.009
16	S-230517c-12	33	357	147	0.41	0.730	0.010
17	S-230517c-13	70	813	167	0.21	0.770	0.010
18	S-230517c-14	33	344	70	0.20	0.808	0.011
19	S-230517c-15	26	257	59	0.23	0.863	0.011
20	S-230517c-16	27	253	56	0.22	0.936	0.013
21	S-230517c-17	10	65	34	0.53	1.333	0.019
22	S-230517c-18	39	348	90	0.26	0.959	0.013
23	S-230517c-19	23	110	91	0.83	1.792	0.024
24	S-230517c-20	31	315	108	0.34	0.804	0.011
25	S-230517c-21	30	302	114	0.38	0.846	0.011
26	S-230517c-22	27	281	88	0.31	0.787	0.010
27	S-230517c-23	28	299	74	0.25	0.780	0.010
28	S-230517c-24	43	451	45	0.10	0.860	0.011
29	S-230517d-01	86	897	262	0.29	0.784	0.010
30	S-230517d-02	493	1011	276	0.27	10.172	0.127
31	S-230517d-03	161	394	160	0.41	6.604	0.083
32	S-230517d-04	71	193	86	0.45	5.350	0.067
33	S-230517d-05	165	425	114	0.27	6.486	0.081
34	S-230517d-06	253	758	24	0.03	5.792	0.073
35	S-230517d-07	85	206	100	0.49	6.658	0.084
36	S-230517d-08	139	230	56	0.24	14.951	0.188
37	S-230517d-09	192	645	12	0.02	4.876	0.062
38	S-230517d-10	108	309	179	0.58	6.851	0.087
39	S-230517d-11	100	184	16	0.09	13.293	0.169
40	S-230517d-12	65	160	79	0.50	6.183	0.079
41	S-230517d-13	30	283	165	0.58	0.801	0.011
42	S-230517d-14	104	809	1084	1.34	0.871	0.011
43	S-230517d-15	8	86	25	0.29	0.908	0.013
44	S-230517d-16	24	183	153	0.84	1.174	0.016
45	S-230517d-17	12	49	51	1.04	2.352	0.037
46	S-230517d-18	24	249	96	0.39	0.949	0.013
47	S-230517d-19	21	212	97	0.46	0.807	0.011

1							
2	S-230517d-20	31	313	111	0.36	0.799	0.011
3	S-230517d-21	15	148	128	0.86	0.704	0.010
4	S-230517d-22	39	419	136	0.32	0.770	0.010
5	S-230517d-23	26	261	114	0.44	0.791	0.011
6	S-230517d-24	30	238	231	0.97	0.915	0.013
7	S-230517e-01	6	59	26	0.45	0.785	0.012
8	S-230517e-02	52	521	319	0.61	0.745	0.010
9	S-230517e-03	17	186	42	0.23	0.894	0.012
10	S-230517e-04	16	172	78	0.45	0.724	0.010
11	S-230517e-05	17	181	59	0.32	0.775	0.010
12	S-230517e-06	24	257	89	0.35	0.759	0.010
13	S-230517e-07	41	405	178	0.44	0.794	0.010
14	S-230517e-08	17	167	71	0.43	1.018	0.013
15	S-230517e-09	14	140	55	0.39	0.807	0.011
16	S-230517e-10	21	214	54	0.25	0.803	0.011
17	S-230517e-11	27	292	31	0.11	0.808	0.011
18	S-230517e-12	34	359	77	0.21	0.809	0.011
19	S-230517e-13	34	351	52	0.15	0.949	0.012
20	S-230517e-14	69	687	235	0.34	0.852	0.011
21	S-230517e-15	11	104	57	0.54	0.766	0.011
22	S-230517e-16	28	308	114	0.37	0.730	0.010
23	S-230517e-17	15	125	45	0.36	1.146	0.016
24	S-230517e-18	43	476	139	0.29	0.736	0.010
25	S-230517e-19	21	224	40	0.18	0.792	0.011
26	S-230517e-20	31	321	81	0.25	0.783	0.010
27	S-230517e-21	22	233	120	0.52	0.720	0.010
28	S-230517e-22	26	255	99	0.39	0.805	0.011
29	S-230517e-23	26	254	175	0.69	0.810	0.011
30	S-230517e-24	48	481	311	0.65	0.731	0.010
31							
32	Carrière le Lorinou						
33	S-140414a-1	25	280	94	0.33	0.741	0.009
34	S-140414a-2	9	96	35	0.37	0.760	0.010
35	S-140414a-3	242	631	189	0.30	6.313	0.076
36	S-140414a-4	12	103	39	0.38	0.977	0.013
37	S-140414a-5	45	476	79	0.17	0.817	0.010
38	S-140414a-6	3	27	13	0.50	0.885	0.017
39	S-140414a-7	36	360	159	0.44	0.772	0.010
40	S-140414a-8	15	169	54	0.32	0.715	0.009
41	S-140414a-9	94	144	84	0.59	13.867	0.168
42	S-140414a-10	30	255	194	0.76	0.909	0.012
43	S-140414a-11	15	143	67	0.47	0.822	0.011
44	S-140414a-12	41	101	68	0.67	5.736	0.071
45	S-140414a-13	22	207	78	0.38	0.840	0.011
46	S-140414a-14	67	117	124	1.06	10.163	0.125
47	S-140414a-15	45	356	130	0.37	1.090	0.014

1							
2	S-140414a-16	214	362	165	0.46	14.056	0.172
3	S-140414a-17	35	80	54	0.68	6.804	0.085
4	S-140414a-18	52	113	55	0.49	8.106	0.100
5	S-140414a-19	133	218	26	0.12	16.275	0.200
6	S-140414a-20	19	164	56	0.34	0.949	0.012
7	S-140414a-21	148	545	73	0.13	4.200	0.052
8	S-140414a-22	20	132	91	0.69	1.268	0.017
9	S-140414a-23	56	470	213	0.45	1.005	0.014
10	S-140414a-24	9	90	28	0.31	0.811	0.011
11	S-140414a-25	16	45	26	0.56	5.017	0.065
12	S-140414a-26	3	34	15	0.46	0.834	0.014
13	S-140414a-27	23	176	73	0.41	1.104	0.014
14	S-140414a-28	195	566	42	0.07	5.907	0.074
15	S-140414a-29	28	235	134	0.57	0.950	0.012
16	S-140414a-30	57	124	56	0.45	8.017	0.102
17	S-140414a-31	14	119	87	0.73	0.935	0.013
18	S-140414a-32	26	179	106	0.59	1.168	0.015
19	S-140414a-33	204	726	270	0.37	3.801	0.046
20	S-140414a-34	191	570	64	0.11	5.336	0.065
21	S-140414a-35	27	232	120	0.52	0.941	0.012
22	S-140414a-36	24	241	46	0.19	0.841	0.011
23	S-140414a-37	18	159	121	0.76	0.797	0.011
24	S-140414a-38	5	40	42	1.05	0.979	0.015
25	S-140414a-39	24	129	146	1.13	1.421	0.018
26	S-140414a-40	30	281	164	0.59	0.807	0.010
27	S-140414a-41	22	57	73	1.29	4.682	0.059
28	S-140414a-42	41	414	196	0.47	0.802	0.010
29	S-140414a-43	13	131	49	0.37	0.845	0.011
30	S-140414a-44	20	185	127	0.69	0.823	0.011
31	S-140414a-45	72	127	48	0.37	14.286	0.175
32	S-140414a-46	32	195	70	0.36	1.617	0.021
33	S-140414a-47	144	357	122	0.34	6.854	0.084
34	S-140414a-48	34	367	152	0.41	0.760	0.010
35	S-140414a-49	12	125	38	0.30	0.783	0.011
36	S-140414a-50	22	222	61	0.27	0.802	0.010
37	S-140414a-51	58	343	131	0.38	1.703	0.021
38	S-140414a-52	9	65	88	1.35	0.882	0.013
39	S-140414a-53	4	42	13	0.31	0.794	0.013
40	S-140414a-54	15	160	39	0.25	0.804	0.011
41	S-140414a-55	27	212	240	1.13	0.838	0.011
42	S-140414a-56	24	232	102	0.44	0.855	0.012
43	S-140414a-57	24	246	52	0.21	0.806	0.011
44	S-140414a-58	2	21	7	0.34	0.912	0.016
45	S-140414a-59	55	138	58	0.42	6.251	0.079
46	S-140414a-60	27	264	120	0.46	0.801	0.011
47	S-140414a-61	124	273	97	0.36	8.212	0.104

1							
2	S-140414a-62	13	138	44	0.32	0.787	0.011
3	S-140414a-63	8	78	37	0.48	0.804	0.012
4	S-140414a-64	20	199	74	0.37	0.814	0.011
5	S-140414a-65	10	64	53	0.82	1.153	0.016
6	S-140414a-66	11	101	39	0.39	0.887	0.012
7	S-140414a-67	69	161	68	0.42	6.961	0.089
8	S-140414a-68	9	85	44	0.52	0.859	0.013
9	S-140414a-69	22	147	100	0.68	1.231	0.016
10	S-140414a-70	6	52	49	0.93	0.874	0.015
11	S-140414a-71	24	239	131	0.55	0.765	0.010
12	S-140414a-72	62	622	112	0.18	0.883	0.011
13	S-140414a-73	44	394	415	1.05	0.776	0.010
14	S-140414a-74	48	552	126	0.23	0.726	0.009
15	S-140414a-75	143	245	153	0.63	12.112	0.144
16	S-140414a-76	19	213	85	0.40	0.727	0.010
17	S-140414a-77	18	162	102	0.63	0.854	0.014
18	S-140414a-78	37	57	32	0.56	13.935	0.172
19	S-140414a-79	60	116	30	0.26	11.560	0.141
20	S-140414a-80	19	191	53	0.28	0.834	0.012
21	S-140414a-81	25	267	14	0.05	0.863	0.012
22	S-140414a-82	58	649	243	0.37	0.711	0.009
23	S-140414a-83	41	186	206	1.11	1.800	0.023
24	S-140414a-84	17	39	35	0.88	6.278	0.083
25	S-140414a-85	43	434	144	0.33	0.824	0.011
26	S-140414a-86	8	68	71	1.05	0.818	0.014
27	S-140414a-87	49	284	164	0.58	1.580	0.021
28	S-140414a-88	12	127	37	0.30	0.769	0.012
29	S-140414a-89	28	56	80	1.42	6.209	0.083
30							
31							
32							
33							
34							
35							
36							
37							
38							
39							
40							
41							
42							
43							
44							
45							
46							
47							
48							
49							
50							
51							
52							
53							
54							
55							
56							
57							
58							
59							
60							

Isotopic Ratios					Apparatus		
Pb206/U238	PropErr2sigAbs.	Rho	Conc.	Pb207/Pb206	PropErr2sigAbs.	Pb206/U238	
0.0932	0.0012	0.97	85	1033	21	575	
0.0948	0.0012	0.93	100	590	24	584	
0.3341	0.0042	0.98	90	2338	18	1858	
0.0938	0.0012	0.96	100	586	23	578	
0.0945	0.0012	0.90	100	570	25	582	
0.0933	0.0012	0.95	101	550	24	575	
0.0847	0.0011	0.94	93	741	24	524	
0.0901	0.0011	0.94	100	550	24	556	
0.0938	0.0012	0.90	95	719	25	578	
0.1007	0.0013	0.96	100	616	23	618	
0.0965	0.0012	0.93	101	573	25	594	
0.0950	0.0012	0.91	95	743	24	585	
0.0964	0.0012	0.95	100	588	24	593	
0.0936	0.0012	0.93	100	564	25	577	
0.0888	0.0011	0.93	99	585	24	548	
0.0985	0.0012	0.94	100	593	23	605	
0.0974	0.0012	0.92	101	566	25	599	
0.0985	0.0012	0.92	101	578	25	606	
0.0980	0.0012	0.92	100	604	25	603	
0.0978	0.0012	0.90	99	622	26	602	
0.0919	0.0012	0.90	99	593	25	567	
0.0909	0.0012	0.93	99	595	25	561	
0.0936	0.0012	0.87	98	636	27	577	
0.0953	0.0012	0.91	100	594	26	587	
0.0817	0.0010	0.94	83	1025	23	506	
0.0869	0.0011	0.95	96	661	23	537	
0.0964	0.0012	0.94	100	592	24	593	
0.0976	0.0012	0.95	100	608	24	600	
0.0977	0.0012	0.97	100	615	23	601	
0.0978	0.0012	0.95	100	595	24	602	
0.0982	0.0012	0.94	97	704	23	604	
0.0941	0.0012	0.95	100	585	24	580	
0.0926	0.0012	0.94	100	582	24	571	
0.0901	0.0011	0.96	99	598	23	556	
0.0948	0.0012	0.92	95	743	25	584	
0.0943	0.0012	0.96	97	676	23	581	
0.1075	0.0014	0.93	97	739	24	658	
0.0966	0.0012	0.97	100	584	23	595	
0.0962	0.0012	0.93	100	595	25	592	
0.0913	0.0011	0.95	99	590	24	564	
0.0860	0.0011	0.93	98	579	25	532	
0.0880	0.0011	0.93	98	587	24	544	
0.1438	0.0018	0.95	96	1003	22	866	

1							
2	0.0923	0.0012	0.93	99	607	25	569
3	0.0937	0.0012	0.93	100	578	25	577
4	0.0850	0.0011	0.90	97	625	25	526
5							
6	0.0944	0.0012	0.97	99	605	23	581
7	0.0889	0.0011	0.95	96	664	23	549
8	0.1150	0.0014	0.95	99	727	23	702
9							
10	0.0983	0.0012	0.96	100	601	23	605
11	0.0787	0.0010	0.97	58	1922	19	489
12	0.0980	0.0012	0.95	100	612	23	603
13							
14	0.0975	0.0012	0.96	100	612	23	600
15	0.0976	0.0012	0.93	101	584	24	601
16	0.0922	0.0012	0.93	98	630	24	568
17							
18	0.0938	0.0012	0.95	100	588	24	578
19	0.0871	0.0011	0.94	99	576	24	539
20	0.0880	0.0011	0.93	98	611	24	544
21							
22	0.0858	0.0011	0.94	92	776	23	531
23	0.0971	0.0012	0.94	99	617	24	597
24	0.1008	0.0013	0.94	98	678	24	619
25							
26	0.1066	0.0013	0.93	97	733	24	653
27	0.1428	0.0018	0.88	100	860	25	861
28	0.1122	0.0014	0.94	100	675	24	685
29							
30	0.1743	0.0022	0.92	99	1056	23	1036
31	0.0944	0.0012	0.93	97	666	24	581
32	0.0964	0.0012	0.92	95	731	24	593
33							
34	0.0958	0.0012	0.92	100	588	25	590
35	0.0948	0.0012	0.93	100	591	25	584
36	0.1006	0.0012	0.93	98	675	24	618
37							
38	0.0949	0.0012	0.98	99	602	22	584
39	0.4497	0.0056	0.99	98	2498	17	2394
40	0.3763	0.0047	0.99	100	2061	18	2059
41							
42	0.3384	0.0042	0.98	100	1875	19	1879
43	0.3709	0.0046	0.99	99	2055	18	2034
44	0.3395	0.0042	0.99	97	2011	18	1884
45	0.3753	0.0047	0.98	99	2080	18	2054
46							
47	0.5480	0.0068	0.98	100	2809	17	2817
48	0.3069	0.0038	0.97	95	1884	19	1725
49							
50	0.3031	0.0038	0.98	84	2497	18	1707
51	0.5178	0.0064	0.98	100	2709	17	2690
52	0.3660	0.0045	0.97	100	1994	19	2010
53							
54	0.0961	0.0012	0.94	99	620	24	592
55	0.0987	0.0012	0.95	95	742	23	607
56	0.0910	0.0011	0.85	86	997	26	561
57							
58	0.1109	0.0014	0.91	86	1117	23	678
59	0.2064	0.0026	0.82	97	1261	27	1210
60	0.0908	0.0011	0.92	83	1089	23	560
	0.0966	0.0012	0.92	99	625	25	595

1							
2	0.0968	0.0012	0.93	100	601	25	595
3	0.0876	0.0011	0.88	100	539	27	541
4	0.0918	0.0011	0.92	98	634	24	566
5							
6	0.0966	0.0012	0.91	100	582	25	594
7	0.1056	0.0013	0.91	98	703	25	647
8	0.0945	0.0012	0.83	99	613	29	582
9							
10	0.0914	0.0011	0.97	100	573	23	564
11	0.0882	0.0011	0.94	84	1029	22	545
12	0.0895	0.0011	0.93	100	555	25	553
13							
14	0.0931	0.0012	0.92	98	619	25	574
15	0.0937	0.0012	0.95	101	557	24	578
16	0.0972	0.0012	0.96	101	575	23	598
17							
18	0.0946	0.0012	0.94	82	1148	22	583
19	0.0964	0.0012	0.91	99	630	25	593
20	0.0975	0.0012	0.94	100	595	24	600
21							
22	0.0980	0.0012	0.95	100	595	24	603
23	0.0979	0.0012	0.96	100	600	24	602
24							
25	0.0981	0.0012	0.96	89	934	22	603
26	0.0977	0.0012	0.96	96	717	23	601
27	0.0940	0.0012	0.88	100	569	26	579
28	0.0879	0.0011	0.94	98	613	24	543
29							
30	0.1184	0.0015	0.89	93	935	25	721
31	0.0896	0.0011	0.95	99	589	24	553
32	0.0964	0.0012	0.93	100	589	25	594
33							
34	0.0959	0.0012	0.94	101	576	24	590
35	0.0895	0.0011	0.91	100	544	26	552
36	0.0975	0.0012	0.91	100	600	25	600
37	0.0897	0.0011	0.92	92	790	24	554
38							
39	0.0894	0.0011	0.93	99	579	24	552
40							
41							
42	0.0894	0.0011	0.94	91	609	24	552
43	0.0920	0.0011	0.88	94	602	26	567
44							
45	0.3623	0.0043	1.00	97	2048	18	1993
46	0.1104	0.0013	0.91	90	747	25	675
47	0.0981	0.0012	0.98	98	618	23	603
48							
49	0.1037	0.0013	0.65	95	671	39	636
50	0.0952	0.0011	0.96	104	562	23	586
51	0.0892	0.0011	0.92	103	536	26	551
52							
53	0.5555	0.0067	0.99	107	2663	17	2848
54	0.1030	0.0012	0.94	85	741	23	632
55	0.0987	0.0012	0.90	98	619	25	607
56							
57	0.3582	0.0043	0.97	104	1898	19	1974
58	0.1006	0.0012	0.94	99	626	24	618
59	0.4482	0.0054	0.98	95	2502	18	2387
60	0.1230	0.0015	0.96	100	750	23	748

1							
2	0.5105	0.0061	0.98	94	2824	17	2659
3	0.3770	0.0046	0.97	98	2110	19	2062
4	0.4146	0.0050	0.97	99	2249	18	2236
5	0.5637	0.0068	0.98	99	2901	17	2882
6	0.1118	0.0014	0.92	104	660	24	683
7	0.2718	0.0033	0.97	85	1834	19	1550
8	0.1349	0.0016	0.92	93	874	24	816
9	0.1120	0.0014	0.89	88	779	25	684
10	0.0943	0.0012	0.88	85	686	26	581
11	0.3251	0.0039	0.93	99	1832	20	1814
12	0.0953	0.0012	0.73	81	725	33	587
13	0.1255	0.0015	0.93	104	734	24	762
14	0.3486	0.0042	0.96	96	1999	19	1928
15	0.1099	0.0013	0.92	96	698	24	672
16	0.4147	0.0050	0.95	100	2230	19	2236
17	0.1038	0.0013	0.90	81	784	25	637
18	0.1299	0.0016	0.95	101	781	23	788
19	0.2606	0.0031	0.99	86	1728	19	1493
20	0.3359	0.0041	0.99	99	1884	18	1867
21	0.1104	0.0013	0.95	101	669	23	675
22	0.1010	0.0012	0.95	101	616	23	620
23	0.0980	0.0012	0.92	106	566	25	603
24	0.1136	0.0014	0.81	100	691	29	694
25	0.1502	0.0018	0.95	101	889	23	902
26	0.0968	0.0012	0.95	96	621	24	595
27	0.2947	0.0036	0.96	88	1884	20	1665
28	0.0946	0.0011	0.96	89	658	23	582
29	0.0960	0.0012	0.90	80	736	25	591
30	0.0948	0.0012	0.90	82	708	25	584
31	0.4958	0.0060	0.98	90	2898	17	2596
32	0.1590	0.0019	0.94	92	1036	22	951
33	0.3765	0.0045	0.98	97	2126	18	2060
34	0.0896	0.0011	0.95	84	659	23	553
35	0.0947	0.0012	0.88	97	603	27	583
36	0.0971	0.0012	0.92	100	600	25	597
37	0.1593	0.0019	0.96	84	1135	21	953
38	0.1036	0.0013	0.85	95	667	28	635
39	0.0975	0.0012	0.75	105	569	33	600
40	0.0949	0.0012	0.91	89	657	25	584
41	0.1010	0.0012	0.92	102	610	25	620
42	0.0991	0.0012	0.89	88	695	25	609
43	0.0985	0.0012	0.93	104	580	25	606
44	0.1061	0.0013	0.69	95	685	36	650
45	0.3673	0.0044	0.95	100	2007	19	2017
46	0.0977	0.0012	0.92	103	585	25	601
47	0.4180	0.0050	0.95	100	2258	19	2251

1							
2	0.0958	0.0012	0.89	100	589	26	590
3	0.0983	0.0012	0.85	104	580	28	604
4	0.0966	0.0012	0.90	92	644	25	594
5	0.1292	0.0016	0.86	102	766	27	783
6	0.1056	0.0013	0.87	101	638	27	647
7	0.3884	0.0047	0.94	101	2098	20	2115
8	0.1016	0.0012	0.75	96	649	32	624
9	0.1317	0.0015	0.87	92	863	25	797
10	0.1010	0.0012	0.70	88	701	34	620
11	0.0936	0.0011	0.86	100	577	27	577
12	0.1027	0.0012	0.91	92	687	24	630
13	0.0921	0.0011	0.89	88	644	25	568
14	0.0893	0.0010	0.92	97	566	25	551
15	0.4940	0.0056	0.96	98	2633	18	2588
16	0.0871	0.0010	0.84	86	625	27	538
17	0.0978	0.0012	0.71	83	721	34	601
18	0.5518	0.0063	0.93	106	2682	19	2833
19	0.4700	0.0054	0.93	94	2638	18	2483
20	0.0983	0.0011	0.83	92	658	28	605
21	0.1001	0.0011	0.84	89	693	27	615
22	0.0863	0.0010	0.89	89	597	25	533
23	0.1758	0.0020	0.88	100	1049	24	1044
24	0.3550	0.0041	0.87	94	2074	22	1959
25	0.0970	0.0011	0.88	90	662	26	597
26	0.0986	0.0012	0.68	99	610	36	606
27	0.1515	0.0017	0.86	84	1086	25	909
28	0.0928	0.0011	0.76	94	607	31	572
29	0.3647	0.0042	0.85	100	2007	22	2004
30							
31							
32							
33							
34							
35							
36							
37							
38							
39							
40							
41							
42							
43							
44							
45							
46							
47							
48							
49							
50							
51							
52							
53							
54							
55							
56							
57							
58							
59							
60							

1			
2	ent Ages		
3	PropErr2sigAbs. Pb207/U235 PropErr2sigAbs.		
4			
5			
6	7	677	6
7	7	585	6
8			
9	20	2096	11
10	7	580	6
11	7	580	6
12	7	570	6
13			
14	6	567	6
15	7	555	6
16	7	607	6
17			
18	7	618	6
19	7	589	6
20	7	618	6
21	7	592	6
22	7	574	6
23	7	555	6
24	7	603	6
25	7	592	6
26	7	600	6
27	7	603	6
28	7	606	6
29	7	572	6
30	7	568	6
31	7	589	7
32	7	588	6
33			
34	6	612	6
35	6	561	6
36	7	593	6
37	7	602	6
38	7	604	6
39	7	600	6
40	7	625	6
41	7	581	6
42	7	573	6
43	7	564	6
44	7	618	6
45	7	601	6
46	8	677	7
47	7	592	6
48	7	593	6
49	7	569	6
50			
51	6	541	6
52	7	552	6
53			
54	10	905	8
55			
56			
57			
58			
59			
60			

1			
2	7	577	6
3	7	577	6
4	6	545	6
5	7	586	6
6	7	572	6
7	8	708	7
8	7	604	6
9	6	836	7
10	7	604	6
11	7	602	6
12	7	597	6
13	7	581	6
14	7	580	6
15	6	546	6
16	6	557	6
17	6	580	6
18	7	601	6
19	7	632	6
20	8	671	7
21	10	860	8
22	8	683	7
23	12	1042	9
24	7	599	6
25	7	622	6
26	7	589	6
27	7	585	6
28	7	630	6
29	7	588	6
30	25	2451	12
31	22	2060	11
32	20	1877	11
33	22	2044	11
34	20	1945	11
35	22	2067	11
36	28	2812	12
37	19	1798	11
38	19	2092	11
39	27	2701	12
40	21	2002	11
41	7	598	6
42	7	636	6
43	7	656	7
44	8	789	7
45	14	1228	11
46	7	677	7
47	7	601	6

1			
2	7	597	6
3	7	541	6
4	7	580	6
5	7	592	6
6	8	660	7
7	7	588	7
8	7	565	6
9	7	648	6
10	7	553	6
11	7	583	6
12	7	573	6
13	7	593	6
14	7	713	7
15	7	601	6
16	7	599	6
17	7	601	6
18	7	602	6
19	7	678	6
20	7	626	6
21	7	577	6
22	6	557	6
23	9	775	8
24	7	560	6
25	7	593	6
26	7	587	6
27	7	551	6
28	7	600	6
29	7	602	6
30	7	557	6
31			
32			
33	6	563	5
34	7	574	6
35	21	2020	11
36	8	692	7
37	7	606	6
38	8	644	9
39	7	581	6
40	6	548	6
41	28	2741	11
42	7	656	6
43	7	609	6
44	20	1937	11
45	7	619	6
46	24	2450	11
47	9	748	7

1			
2	26	2754	12
3	21	2086	11
4	23	2243	11
5	28	2893	12
6	8	678	7
7	17	1674	10
8	9	831	7
9	8	707	7
10	7	603	6
11	19	1822	11
12	7	616	8
13	9	755	7
14	20	1962	11
15	8	678	6
16	23	2233	11
17	7	670	7
18	9	786	7
19	16	1593	10
20	20	1875	10
21	8	674	6
22	7	620	6
23	7	595	6
24	8	693	8
25	10	898	8
26	7	601	6
27	18	1764	11
28	7	598	6
29	7	622	6
30	7	610	6
31	26	2769	12
32	11	977	8
33	21	2093	11
34	6	574	6
35	7	587	6
36	7	598	6
37	11	1010	8
38	7	642	7
39	7	593	7
40	7	599	6
41	7	618	6
42	7	627	6
43	7	600	6
44	8	658	9
45	21	2012	11
46	7	597	6
47	23	2255	11

1			
2	7	590	6
3	7	599	6
4	7	605	6
5	9	779	8
6	7	645	7
7			
8	22	2106	11
9	7	629	7
10	9	815	7
11	7	638	8
12	6	577	6
13	7	642	6
14	6	583	6
15	6	554	5
16	24	2613	11
17	6	555	6
18	7	627	8
19	26	2745	12
20	23	2569	11
21	7	616	6
22	7	632	6
23	6	546	5
24	11	1045	8
25	19	2015	12
26	6	610	6
27	7	607	8
28	10	963	8
29	6	579	7
30	20	2006	12
31			
32			
33			
34			
35			
36			
37			
38			
39			
40			
41			
42			
43			
44			
45			
46			
47			
48			
49			
50			
51			
52			
53			
54			
55			
56			
57			
58			
59			
60			

		Pb207/U235	ErrAbs	Pb206/U238	ErrAbs	rho
1						
2						
3	Pleso 1	0.3947	0.0054	0.05345	0.00067	0.92
4	Pleso 2	0.3996	0.0064	0.05317	0.00068	0.79
5						
6	Pleso 3	0.3966	0.0053	0.05375	0.00067	0.94
7	Pleso 4	0.3956	0.0053	0.05384	0.00067	0.93
8	Pleso 5	0.3981	0.0053	0.05342	0.00067	0.94
9						
10	Pleso 6	0.3966	0.0053	0.05321	0.00066	0.92
11	Pleso 7	0.3938	0.0053	0.05377	0.00066	0.92
12	Pleso 8	0.3892	0.0052	0.05379	0.00067	0.93
13						
14	Pleso 9	0.3924	0.0053	0.05329	0.00066	0.92
15	Pleso 10	0.3920	0.0054	0.05336	0.00067	0.91
16	Pleso 11	0.3943	0.0052	0.05371	0.00067	0.94
17						
18	Pleso 12	0.3889	0.0051	0.05374	0.00067	0.94
19	Pleso 13	0.3895	0.0053	0.05364	0.00067	0.92
20	Pleso 14	0.3918	0.0051	0.05378	0.00065	0.93
21						
22	Pleso 15	0.3905	0.0050	0.05375	0.00065	0.94
23	Pleso 16	0.3908	0.0052	0.05377	0.00065	0.91
24	Pleso 17	0.3895	0.0051	0.05379	0.00065	0.93
25						
26	Pleso 18	0.3924	0.0054	0.05388	0.00065	0.88
27	Pleso 19	0.3949	0.0049	0.05364	0.00064	0.96
28	Pleso 20	0.3949	0.0050	0.05370	0.00064	0.94
29						
30	Pleso 21	0.3916	0.0049	0.05369	0.00064	0.95
31	Pleso 22	0.3944	0.0050	0.05349	0.00064	0.94
32	Pleso 23	0.3939	0.0051	0.05383	0.00064	0.92
33						
34	Pleso 24	0.3962	0.0049	0.05392	0.00065	0.97
35	Pleso 25	0.3945	0.0049	0.05384	0.00064	0.95
36	Pleso 26	0.3998	0.0050	0.05351	0.00064	0.95
37						
38	Pleso 27	0.3941	0.0050	0.05369	0.00064	0.93
39	Pleso 28	0.3928	0.0050	0.05377	0.00064	0.93
40	Pleso 29	0.3872	0.0050	0.05365	0.00065	0.95
41						
42	Pleso 30	0.3927	0.0053	0.05344	0.00065	0.91
43	Pleso 31	0.3939	0.0051	0.05379	0.00065	0.94
44	Pleso 32	0.3909	0.0052	0.05369	0.00065	0.90
45	Pleso 33	0.3932	0.0053	0.05376	0.00065	0.89
46						
47	Pleso 34	0.3955	0.0050	0.05379	0.00062	0.91
48	Pleso 35	0.3947	0.0053	0.05377	0.00061	0.85
49	Pleso 36	0.3945	0.0053	0.05342	0.00061	0.84
50						
51						
52						
53						
54						
55						
56						
57						
58						
59						
60						